Medical Engineering and Physics, Volume number 30, Issue 10, December 2008, pp. 1209-1226
DOI: 10.1016/j.medengphy.2008.09.007

Fracture of bone tissue: the 'hows' and the 'whys'

H. S. Gupta[1] & P. Zioupos[2]*

[1] *Biomaterials Department, Max Planck Institute of Colloids and Interfaces, 14424 Potsdam, Germany*

[2] *Biomechanics Laboratories, Cranfield University, Shrivenham SN6 8LA, UK.*

Abstract

The mechanical performance of bone is of paramount importance for the quality of life we experience. The structural integrity of bone, its hierarchical structure, organisation and its physicochemical constitution, all influence its ability to withstand loads, such as those seen occasionally in everyday life loading scenarios, which are either above the norm, prolonged, or repetitive. The present review explores three interconnected areas of research where significant progress has been made lately: (i) The recorded mechanical behaviour of bone and the way it fails; (ii) the inner architecture, organisational, hierarchical structure of bone tissue, and (iii) the bone properties at the micro/nano structural and biophysical level. Exercising a line of thought along a structure/function based argument we advance from 'how' bone fractures to 'why' it fractures, and we seek to obtain a fresh insight in this field.

Keywords: Bone; Fracture; Mechanisms; Properties; Structure; Hierarchy; Organisation

* Corresponding author: Tel.. +44 1793 785932; fax. +44 1793 763076. *E-mail address*: p.zioupos@cranfield.ac.uk (P.Zioupos)

1. Introduction

The mechanical performance of bone is of paramount importance for the quality of life we experience, as fractures are painful debilitating events. Some fractures are quite obviously due to the fact that bone is subject to loads that exceed certain threshold levels (in terms of stress or damage), that may also be prolonged (creep), or repetitive (fatigue). Others are caused by bone being structurally compromised as a result of disease, ageing, surgical intervention, pharmaceutical treatments, poor diet, lack of exercise, and so forth. In all cases some sense can be made by invoking either material/ engineering principles to explain the effects of overload, or structure/function relationships[1] to grapple with the effects of a materially and structurally compromised tissue.

2. How bone breaks

There is a consensus regarding the various stages leading to and during fracture of bone, but what is still debated is the relative importance of the various phases in determining the final failure outcome[2]. The stress/strain curve (in tension) for bone as a material shows a (macroscopically) linear phase followed by a 'knee' region where the material yields and then a region of strain hardening (which can

be shorter or longer depending on the circumstances) followed by sudden catastrophic failure. This applies to tests as seen in the lab on material testing specimens. In terms of σ/ε behaviour though the description and analysis of the failure of bone is partitioned in 3 domains, as shown in Fig. 1. In phase-I the material deforms reversibly with little obvious residual damage, while in phase II (the elastic-continuum damage mechanics domain) where the material is still structurally integrated but absorbs energy by developing diffuse microcracking damage at the expense of stiffness and residual strength. In phase III, the fracture mechanics (FM) realm, energy is absorbed at and next to the final fracture surface; the amount of energy depending crucially on the properties of the final fracture plane and the overall number of such planes and/or fragments.

The toughness of a material is defined in terms of stress or energy related requirements to run a crack through the material. Stress-based criteria, such as the stress intensity factor (K_c) postulate that fracture is initiated when the concentration of stress at the crack tip reaches a critical value. Energy-based approaches, which either measure the critical strain energy release rate G_c (or J, for non-linear effects) or the work to fracture of a specimen W_f, determine critical levels of energy per unit area necessary for fracture. In this field it has become quite clear recently that modern composites (and for that matter bone[3] and other biological hard tissues) show weak interlamellar interfaces[4], which are able to absorb energy and/or divert a crack and in this way deter the onset and growth of fracture. Further, it is now increasingly clear that initiation of cracks in biomineralized tissues is far less important that their propagation, since biological tissues utilise a number of tricks like crack diversion/deflection, fibre pull-out, crack and/or matrix bridging[5, 6] to increase the required amount of energy to fracture. Increasingly, nowadays, emphasis is placed in studying the route of propagation of major cracks[7-9], and the relevant intrinsic toughening mechanisms that are associated with this propagation.

The stress based fracture mechanics (FM) answer for the increased toughness of some challenging biological materials like deer antler[10] (which is a low mineralized bone tissue) was the introduction of the crack growth resistance curves K_R. It consists of quantifying the critical stress intensity factor not only at the start (K_C) when the macrocrack sets off, but also as it makes its way through the material (K_R). In brittle materials the K_R curve is flat, K is constant and, therefore, there is little to deter the crack in its growth. In tough solids, K_R increases with the crack length, especially if there is microcracking at the crack tip, and the crack finds considerable resistance to its advance. Vashishth *et al.*[10] used compact tension specimens from the antlers of red deer to monitor crack propagation via gauges attached onto the specimens and used Scanning electron microscopy (SEM) to count the number of microcracks, with lengths between 100-250 μm. A linear increase of K_R with crack length was observed and a 20% increase in the length of the crack nearly doubled the stress intensity factor. At the same time more microcracks were present in the fracture propagation (K_R) specimens than in the fracture initiation (K_c) ones. Microcracks were seen both ahead and behind the tip of the propagating macrocrack. The authors explained the increase in toughness of antler bone by the

nucleation, growth and coalescence of the observed microcracks, which were responsible for the stable progress of fracture by absorbing energy away from the main crack itself. Ritchie and co-workers[11-16] (add Koerster references) have carried this approach much further, by a combination of fracture mechanics experimentation, modelling and high resolution scanning electron microscopy. What they found was that ligament, or crack bridging, by collagen fibrils spanning the width of a propagated microcrack, results in a progressively increasing fracture resistance in bone.

A combination of K_C and K_R data can explain quite a few naturally occurring variations in bone properties. Zioupos & Currey[17] showed that the initiation fracture toughness (K_C) of human femoral cortical bone, measured by single edge notch bending tests, reduced considerably between the ages of 35 and 92 in healthy male subject (Fig. 2a). Ritchie, Nalla *et al.*[11-16] and co-workers took this a step further showing that both the initiation toughness (K_C) and the growth toughness (K_R) of ageing human bone deteriorate in a similar fashion over the same range of age values (Fig. 2b). They made an effort to apportion relative importance in the various mechanisms that operate at the crack tip (microcracking, fibre pullout, crack bridging etc.) to have the desirable toughening effect. They also made a further distinction between two classes of toughening mechanisms. intrinsic, which are microstructural damage mechanisms that operate ahead of the crack tip and extrinsic mechanisms, which act to 'shield' the crack from the applied driving force and operate principally in the wake of the crack.

By means of controlled crack extension experiments at the lamellar level in osteonal bone, Peterlik *et al.*[4] looked at the strain energy release rate as a function of crack orientation relative to the collagen fibril axis. Using the same sample for repeated loading/unloading measurements enabled directional effects on the toughness of bone to be measured. The fracture process is dependent on the direction of travel of the crack, being either brittle (in the longitudinal direction) or deflected (in the tangential direction) or toughened by microcracking (in the radial direction) (Fig. 3). The microstructural origins of this phenomena lie in the progressively varying fibril angles as proposed by the twisted and rotated plywood models of lamellar bone (see subsequent sections). These results provide evidence of an energy-based understanding of a self toughening (crack growth resistant) fracture process (during propagation) similar to the one described for antler bone[18]. The energy based FM approach of Peterlik *et al.*[4] has certain conceptual and practical advantages over the previous FM stress related one. In composites science, engineering toughness is increasingly nowadays defined in terms of energy absorbing capacity, the methods to determine this being reliable simple and consistent. At the same time the unpredictable events at the crack tip, which give rise to the stress field and determine the stress intensity factor, can be hardly described in terms of equations that pertain to idealised elastic conditions that simply do not exist.

FM approaches have proved quite popular, but suffer from another quite unexpected effect. they are restricted to the quasistatic testing range. Many physiological fractures happen as a result of prolonged

loading (creep), repetitive loading (fatigue), or occur at high strain rates (impact). Work of fracture measurements (W_f) are carried out by measuring the energy absorbed to fracture a certain cross sectional area in tests where the ligament of tissue designed to rupture is in the shape of a chevron notch. Because the notch width increase as the fracture front advances the test specimen geometry itself usualyl allows the process to stay in the stable mode as long as possible. In this sense one finds it is much easier to control the tests even at high strain rates.

Currey and co-workers looked at two different effects by using W_f and Charpy impact tests. They measured the W_f values of human femoral samples and demonstrated a 50% reduction of toughness with age[19] between 25 and 80 yrs old. Measurements for the energy absorption capacity of similar specimens at high speeds were obtained by use of a Hounsfield plastics Charpy impact tester. The two data sets showed a very good correlation (Fig. 4a) over a wide range of ages. The young bone in particular, which is less mineralised was especially tough in impact. Although the energy consumed in impact is overall much higher than the specific energy in W_f tests the two values increased hand in hand. This result is reassuring, because it shows that an appreciation of toughening effects at high strain rates can result from simple studies by use of much slower test methods. However, more importantly the fact the specimens used in the two tests were different, but originating from the same individual, showed that the origins of the toughness quantified by either method lie in the intrinsic properties of the mineralized matrix itself and is related to age and other deteriorating bone matrix material physicochemical events.

In the second W_f application the same workers examined deformation rate effects in a group of different animal bone materials[18]. Specimens were obtained from a bovine femur (of typical plexiform architecture), from the femur of a tiger (of typical osteonal architecture) and from the naturally tough material of the antlers of red deer (*Cervus elaphus*) which in life experiences loading in impact. The tests were performed at cross-head speeds varying between 0.05 mm min^{-1} and 200 mm min^{-1} in a materials testing machine and the data was supplemented by tests in impact. Two aspects of the materials' toughness are evident in Fig. 4b. The naturally tough antler bone showed a tendency to dissipate more energy to fracture per unit area as the strain rate increased (an order of magnitude more energy in impact than in quasi-static loading). On the other hand, the three quasi-brittle 'ordinary' bones (human, bovine and tiger) produced similar values for W_f at all deformation rates, including impact for those tests that could be completed successfully. One way of looking at this data is that the W_f produces a material property constant for the 'ordinary' bones, but it showed a rate depended property for the naturally tough bone. A second aspect of toughness was shown by the percentages of successfully completed tests, that is tests that failed as they meant to do in a ductile mode. While antler bone showed no ductile to brittle transition and was able to fail non-catastrophically even in impact, the ordinary bones started showing catastrophic failures at rates above 5 mm min^{-1} (bovine and human) and above 50 mm min^{-1} (tiger femur).

Ductile-to-brittle transition in material behaviour of human femoral cortical bone with strain rate was also observed lately in standard tensile and compressive tests to failure by Hansen *et al.*[18]. These tests on standard material testing un-notched specimens produce σ/ε curves and are suitable for demonstrating the pre-failure microcracking damage absorbing characteristics of bone (phase I-II, Fig. 1). Bone mechanical properties are typically evaluated at relatively low strain rates. However, the strain rate related to traumatic failure is likely to be orders of magnitude higher and this higher strain rate is likely to affect the mechanical properties. Hansen *et al.*[18] tested femoral cortical bone at strain rates ranging between [0.14-29.1 s^{-1}] in compression and [0.08-17 s^{-1}] in tension (Fig. 5) and compared the results with a broad review of all the related literature. Across this strain range, Young's modulus generally increased for both tension and compression. Strength and strain at maximum load increased slightly in compression and decreased (for strain rates beyond 1 s^{-1}) in tension. Stress and strain at yield decreased (for strain rates beyond 1 s^{-1}) for both tension and compression. There seemed to be in general a relatively simple linear relationship between yield properties and strain rate, but the relationships between post-yield properties and strain rate were more complicated and indicated that strain rate has a stronger effect on post-yield deformation than on initiation of yielding. The behaviour seen in compression is broadly in agreement with past literature, while the behaviour observed in tension showed a clear ductile to brittle transition at moderate to high strain rates.

A combination of methods was employed recently to explore the relative importance of phases I-II to phase III (Fig. 1) in bones over a wide range of varying mineral content[20, 21]. Using a simple technique, like adding a notch, which serves to concentrate the stress and check the notch sensitivity of various bone analogues, the authors showed that the post yield behaviour of bone is linked to the mineral content. They argued that antler is practically notch insensitive and possesses probably the lowest mineralisation level in nature, below which no further evolutionary advantage is to be gained or needed by reducing the mineral content any further because any further reduction in mineral content would reduce the stiffness without much increasing the toughness. The literature on antler bone mechanics is very useful because it helps to pose all these awkward questions that have no answer in conventional thinking. It also shows that the pre-failure damage tolerance of bone, although more difficult to quantify, is the most determinant factor in defining the toughness of the material in health, disease and in various exotic bone analogues[22-26].

2. Hierarchical structure and composite mechanics

In order to understand the origins of the high toughness and stiffness of bone, and the reasons for its alterations with age and disease, we have to consider the full complexity of the hierarchical architecture[1, 27] from the macro- to the micro-scale and the mechanical properties of the various constituents at each level. The heterogeneity of bone at the meso- and microscale has a direct influence on growth of cracks within bone and on the failure process (Fig.6).

2.1 Macrostructure: Cortical and Cancellous Bone.

At the macrostructural level, bone is divided into the cortical (or compact) and cancellous (or trabecular) types. The two types are most easily distinguished by their degree of porosity or density[28, 29], true differentiation comes from histological evaluation of the tissue's microstructure. In an intermediate form, compact coarse-cancellous bone[30, 31] differentiation between the two types of bone is difficult. This tissue consists of cortical bone wrapped around older cancellous bone and has irregular, sinuous convolutions of lamellae.

It is still a matter for debate whether (i) cortical and cancellous bone matrices consist of the same material[28, 32-34] (only differentiated by variable porosity or apparent density), or (ii) have intrinsically different mechanical properties[35-39]. Nanoindentation studies have shown that on average the modulus and hardness of the two tissues types are similar[40]. However, since cancellous bone material is much more active metabolically, is remodelled more often than cortical bone, and is therefore "younger" on average than cortical bone[41], mechanical measurements at the macroscale deliver slightly lower values of moduli for cancellous bone tissue compared to cortical bone. Cancellous bone, can be described in terms of structural and material properties[38]. The first are defined as the extrinsic properties of both trabeculae and pores, whereas *material* properties are the properties of the trabecular struts and plates.

As different bone types and regions in the same bone organ have differing mineralization level, porosity and collagen matrix structure, it is difficult to predict micro-properties *in vivo*[42, 43] by measuring mechanical properties at the macrostructural level. Mechanical properties of cortical and cancellous bone at the macrostructural level vary from one bone to another as well as within different regions of the same bone[44, 45]. Cancellous bone shows a wide range of apparent density values (apparent density is defined as mass of sample / (total volume of sample including both voids *and* tissue). However, 70-80% of the variability in its mechanical properties (in the stiffest direction) can be explained in terms of true density variations alone. The variability reduces further when directional effects and anisotropy are accounted for[46, 47]. In all cases technical problems like friction between sample and test grips, and accurate load transfer in the testing setup complicate these measurements[48-50].

However, although cancellous bone has a larger scatter in mechanical properties compared to cortical bone, the intrinsic structure at the lamellar level and at comparable degrees of mineralization are similar. This underlying common microstructure is examined in the next section.

2.2 Microstructure: Osteons and Lamellar Structure.

Haversian Systems. At the level of the entire osteon (Haversian system), our knowledge of the mechanical properties comes mainly from the pioneering work of Ascenzi and coworkers, who examined the mechanical properties in tension[51], compression[52], bending[53] and torsion[54]. Differences were observed in tension for the osteons classified as "longitudinal" (fibrils oriented parallel to the

osteon axis) and "transverse" (fibrils oriented perpendicular to the osteon axis). moduli varied from 12 (longitudinal) to 5.5 (transverse) GPa and strengths from 120 to 102 MPa[51]. Rather surprisingly, isolated osteons in compression[52] were half as stiff (6–7 GPa) but nearly as strong as osteons in tension (110–130 MPa). Bending tests gave even lower values[53] for stiffness of approximately 2–3 GPa and bending strength of 350–390 MPa, while torsional tests[54] gave moduli of 16–20 and strengths of 160–200 MPa. While this dependence of mechanical properties depending on the testing mode may be because different deformation processes in the anisotropic bone tissue are activated, based on the direction of deformation, the bending results especially should be interpreted with caution. The dimensions of the samples used for the bending tests by Ascenzi and co-workers are very short and deep, and in such cases shear deformations cross the sample, which was not considered by these workers, must be included for accurate results.

In terms of failure mechanisms, analysis of fracture surfaces by the Ascenzi group shows that in compression, cross-hatched fissures at 30°–40° appeared and these were not affected by the kind or combination of lamellar architecture, similar to results obtained on compact bone by Mercer *et al.*[55]. As expected, in tension the transverse lamellae failed first and the osteons were kept together only by the longitudinally oriented ones, since clearly fibres are stronger along their main axis than perpendicular to them. Marotti[56] claims that fibres in general follow two patterns which constitute thin and thick lamellae; the thin ones are more oriented and compact, the thick ones are more diverse and sparse (somewhat microporous) in their elements, a classification which differs from that of the Ascenzi group. We believe that the differentiation of osteons based on fiber orientation (the Ascenzi classification) is the correct one, although it has also been recently shown that mineral density can vary within a single lamellae, as described in the next section.

Lamellae. Bone lamellae are ~ 5-8 μm thick[57], and consist of regular arrays of collagen fibrils. Inside a single lamella (as seen in optical and scanning electron microscopy) Giraud-Guille *et al.*[58] and Weiner and co-workers[57, 59, 60] have observed a helicoidal, twisted plywood structure, where successive sheets of sublamellae (with varying thicknesses) have different orientation angles of the fibrils. Giraud-Guille pointed out that these structures are characteristic of the cholesteric liquid crystal mesophases[58, 61]. Weiner, Traub and Wagner have extended this model[57, 59, 60] to a "rotated plywood" structure. In this picture, the mineralized fibril-platelet composite in adjacent sublamellae not only turn in pitch (angle of collagen fibril axis to osteon long axis) but also in "roll", or rotate around the long axis of the fibril itself. Such a model would be useful in diverting extremely small cracks at their incipient growth stage. The osteonal lamellae are wrapped around a central canal, and sequential concentric lamellae have fibre orientations alternating to each other, spiralling around the central canal. Lamellae with alternate orientations are seen as alternately bright, dark, or intermediate in cross-section under a polarized light microscope (PLM) with the intensity of the transmitted light depending on the collagen content, on its degree of alignment, on the presence of a mineral fraction, and on the

orientation of the section[51, 62]. The orientations envisaged in this kind of modelling are transverse, longitudinal, or oblique.

Structural information at this level has been obtained using optical microscopy, X-ray diffraction, and electron microscopy. Mechanical properties of individual lamellae in several orientations are needed to comprehend bone mechanical anisotropy. Some studies which used selective demineralization and acoustic methods have come up with most intriguing theories about the complementary role of the collagen and the mineral[63-65]. These workers have suggested that isolated collagen fibrils are more or less isotropic and by the impregnation of mineral reaches the anisotropic ratios that are known for whole bone (1.7-2.1) in two normal directions. However, their experimental techniques (acoustic microscopy) had a spatial resolution of 60 microns, which is much too low to observe regions of unixaially oriented tissue. Therefore, conflation of data from tissue regions with differently oriented fibrils could be seriously affecting their results Experimental methods that can measure absolute and relative (anisotropy) values for the elastic modulus of microscopic bone tissue in different directions would be invaluable. However, mechanical data at the sub-micron level were unavailable, until recently, when nanoindentation tests were used to measure the hardness and the elastic modulus of single lamellae[66] and small filler particles in resin composites and other dental restoratives[67]. This technique is able to measure mechanical properties with a resolution of better than 1 μm and does not require visual resolution of the indentation. Taking into account the microstructural features of bone, the nanoindentation technique offers a means by which the intrinsic mechanical properties of the individual microstructural components of bone may be measured in a manner which avoids the influences of the inherent defects and heterogeneities in the microstructure and also allows the mechanical properties to be measured in several different directions at the microstructural level.

Using a novel combination of X–ray crystallographic texture measurements with microbeam synchrotron radiation (1 μm beam diameter), Wagermaier *et al.*[68, 69] were able to quantify the fibrillar orientation by tracking changes in mineral c-axis crystallographic texture in “alternate” osteons [as defined by Ascenzi] with sub-lamellar resolution. They found that the fibril orientation was periodic, with a period equal precisely to that of the lamellae, and amplitude of oscillation equal to about 30°-60° (Fig. 7b). What was surprising was that the mean fibril orientation in a single lamella always had the same chirality, indicating that a fine (intralamellar) periodic variation in fibril orientation was superposed on top of an average right handed fibril spiralling. Such a helical and modulated fiber orientation would make crack propagation across the osteon, from the interstitial to the inner Haversian canal, much more difficult and tortuous than the case where all fibers were all parallel to the osteon axis. The osteon may thus serve as a fracture resistant barrier, protecting the integrity of the Haversian canal and its enclosed blood vessels and cells.

However, the lamellae in bone exhibit not only structural anisotropy (from fibre orientation) but also compositional variation[41]. By combining scanning nanoindentation maps of osteons (1 μm resolution)

with quantitative backscattered electron imaging to determine local calcium content, Gupta *et al.*[41] showed that a clear lamellar level modulation of (nanoindentation) elastic modulus and hardness across the osteon (Fig. 7a). Within a single lamella, the variable fiber orientation gives the optical impression of "thick" and "thin" sublamellae, with the "thick" sublamellae having fiber orientation mainly parallel to the osteon axis, and the "thin" sublamellae having fibers at a large angle to the osteon axis. Using position resolved nanoindentation, Rho and coworkers have shown that when only the "thick" sublamellae inside a single lamella were considered, there is a statistically significant decrease in modulus going from the innermost to the outermost lamella [70]. However (using a similar loading protocol and sample geometry to Rho et al 1999), Gupta et al found only a statistically *insignificant* decrease as a function of distance, when moduli was measured in both the "thin" and "thick" sublamellae, in the form of a 2D map with 1 micron effective spatial resolution across the osteon. As the difference between the stiffness of the thin and thick lamellae within a single lamella (15 GPa for the thin lamella versus 20 – 25 GPa for the thick lamella) is much larger than the ~ 2 – 3 GPa variation observed in the thick lamellae across the osteon by Rho et al 1999, it is possible that any statistically significant decrease of "thick" sublamellar moduli in Gupta et al 2006's data was buried in the much larger lamellar level mechanical modulation. The difference between the "thin" and "thick" sublamellae was also measured by Xu *et al.*[71]. Because the mineralized collagen fibrils is anisotropic, with an indentation modulus of about 9–11 GPa transverse to the fibril axis and 20–25 GPa parallel to it[72, 73], one could think that this mechanical modulation arose solely due to the fibril orientation-i.e., similarly mineralized, but differently oriented fibrils in a single lamella. However, by correlating mechanical properties and mineral content at the same point, Gupta *et al.*[41] showed that regions with lower stiffness also had a lower mineral content. Such a periodically mechanically modulated structure may be useful in acting as a set of crack stoppers, preventing microcrack propagation from the more highly mineralized interstitial bone to the inner Haversian system. Microcracks indeed show a tendency to circumvent the osteons along the weak, non-collagenous "cement line" at the border of the osteon and to run between lamellae[74]. A qualitative indication of the modulation of stiffness was observed previously in the ultrasonic measurements of Katz and Meunier[75], where the quantity $(E/\rho)^{1/2}$ was shown to be correlated to the lamellar structure. There is an added difficulty, of course, in interpreting these results in that in acoustic microscopy one needs to avoid the conflation of surface topography with differences in density. This requires careful polishing and surface preparation.

Trabecular Bone. Trabecular bone properties are much easier to study in isolation. However, in spite of several attempts[35, 36, 38, 76] there remains some controversy regarding the value of the elastic modulus of single trabeculae (Table 1). Trabecular bone material properties are important for characterizing various bone pathologies, and the remodelled bone adjacent to various joint implants, because they are affected by disease sooner than cortical bone. In the past it was assumed that individual trabeculae, single osteons, and a thin cortical shell possessed the same mechanical properties as those of large cortical bone specimens regardless of their type or size[75]. However, many

investigators produced values for the elastic modulus of individual trabeculae, single osteons, and a thin cortical shell that were considerably less than that for whole bone[35, 38, 76].

The elastic modulus of cortical bone obtained from micro-bending specimens[35, 36, 38, 76] (dimensions.100×100×1500 μm) is considerably smaller (5.4 GPa) than that of large tensile specimens tested by others[77] (17.1 GPa). The reason for this discrepancy is not clear, but it could arise from difficulties encountered in making accurate mechanical property measurements by bending small specimens. The possible causes include: (i) the influence of microstructural defects such as cement lines and voids (Haversian and Volkmann canals, lacuna, osteocytes, canaliculi) on the measured displacements; (ii) uncertainties in specimen geometry, which are often exacerbated at small scales; and (iii) problems in properly seating and aligning small bending specimens in small test fixtures. A literature survey of measured and estimated values of the modulus of trabecular bone material[35, 38, 66, 76, 78-85] shows that moduli values range from 1 to 20 GPa (Table 1). It has been shown [35, 36, 38, 76] that the relationship derived from this data (between elastic moduli and density in cancellous bone material) could not be extrapolated from similar data from tests on cortical bone material and its density and thus has been concluded that the materials of the two types of bone tissue were intrinsically different. The later studies by use of nanoindentation and by finite element analysis (FEA) simulation suggest that in fact the elastic properties of single trabeculae are very similar to the properties of nearby cortical tissue, though probably slightly lower.

3. Why bone breaks: the biophysical events

3.1 Bone nanostructure: Collagen fibres, fibril arrays, crystals

The most prominent nano-structures are the collagen fibres, surrounded and infiltrated by mineral. The attachment sites of macromolecules onto the collagen framework are not distinctly known, although several immunohistological studies have shown preferential labelling of some macromolecules in a periodic fashion along the collagen molecules and fibres[86].

The three main building materials are crystals, collagen, and non-collagenous organic proteins. Mature crystals are most likely not needle-shaped, but plate-shaped[60]. Plate-like apatite crystals of bone occur within the discrete spaces within the collagen fibrils, thereby limiting the possible primary growth of the mineral crystals, and forcing the crystals to be discrete and discontinuous. The mineral crystals grow with a specific crystalline orientation-the c-axis of the crystals are roughly parallel to the long axis of the collagen fibrils[87]. The average lengths and widths of the plates are 50×25 nm. Crystal thickness is 2 to 3 nm thick[88, 89]. The nanocrystalline bone apatite has small but significant amounts of impurities such as HPO_4, Na, Mg, citrate, carbonate, K, and others whose positions and configurations are not completely known[87]. While the X-ray diffraction pattern is that of hydroxyapatite, the near-absence or absence of the hydroxyl group has been proven repeatedly by chemical methods and FTIR

and NMR spectroscopy[87]. The primary organic component of the matrix is Type I collagen. Collagen molecules secreted by osteoblasts self-assemble into fibrils with a specific tertiary structure having a 67 nm periodicity and 40 nm gaps or holes between the ends of the molecules. Non-collagenous organic proteins, including phosphoproteins, such as osteopontin[90, 91], sialoprotein, osteonectin, and osteocalcin, as well as proteoglycans like decorin[92, 93] may function to regulate the size, orientation, and crystal habit of the mineral deposits. Through chelation of calcium or through enzymatic release of phosphorous from these proteins, they may serve as a reservoir for calcium or phosphate ions for mineral formation. However, additional studies are needed to conclusively define their actions and mechanisms.

As regards the relation between the mineral and organic phase, the degree of extra- versus intrafibrillar mineral is still a matter of debate[57, 65, 94-100]. Estimates have ranged from the majority of mineral being intrafibrillar[100] to the majority being extrafibrillar[65, 94], and this is a significant issue when modelling the mechanical and fracture properties of the collagen nanocomposite[65, 94]. Some recent work considers the entire composite to be an effective "foam" of mineral inside a collagen matrix[65, 94], which blurs the distinction between extra- and intrafibrillar mineral. The mineral particles were shown to be platelike and associated with the low density "gap" zones in collagen fibrils in mineralized turkey leg tendon[57, 59, 101, 102]. More recent bright field transmission electron microscopy of the nanostructure of mineralized collagen fibrils from trabecular bone[99] have both refined and extended this picture. These studies showed that the particles were plate like, consistent with previous work[99]. However, in contrast to the case where mineral platelets are aligned parallel to each other both within as well as between fibrils[60, 102], the TEM results on human bone showed that the mineral platelet orientation in adjacent fibrils is not aligned, and that adjacent fibrils are rotated around their long axis with respect to each other. Therefore, it is expected that, on average, the platelet orientation in groups of adjacent fibrils in sublamellae would show fibre symmetry around the collagen fibril axis.

3.2 Deformation mechanisms

At the time of the previous review in this journal[1], relatively little was known about the deformation mechanisms of the mineralized collagen matrix itself, although localized elastic moduli and hardness values had been reported for trabecular and compact bone using nanoindentation[103]. Since then, advances in experimentation, particularly in the use of synchrotron X-ray diffraction and scattering combined with micromechanical testing[104-107], as well as single molecule force spectroscopic methods [Thompson 2000, Fantner 2005] and nanoindentation with high spatial resolution [Tai Nature Mater 2007] have begun to shed light on this question.. Synchrotron X-ray diffraction enables the simultaneous tracking of deformation in the fibril as well as in the embedded mineral particles, concurrently with the application of macroscopic stress and strain. The principle of the methods is to use the changes in axial periodicity in the collagen fibrils (D–periodicity of ~ 65–67 nm) as a marker of fibrillar strain ε_F. By acquiring small angle X-ray scattering data in real time combined with

microtensile measurements, strain can be followed at the macroscopic and nanoscale levels simultaneously, as shown schematically in Fig. 8. Synchrotron radiation is essential due to its high brilliance, enabling an X-ray spectrum to be obtained in a matter of seconds compared to hours in a lab source. Single molecule force spectroscopy uses a cantilever with an sharp tip (of the order of nanometers) to pull on the long, sometimes amorphous, organic molecules that form a significant part of biomineralized tissues, enabling thereby an estimate of their mechanical properties, Nanoindentation, especially combined with finite element modelling, now can provide models of the deformation processes induced by a sharp, localized force in the biomineralized tissue.

The concept of "sacrificial bonds", which are nonspecific, weak but reformable bonds within the organic component of biomineralized tissues (both bone as well as other materials like abalone nacre), is central to the thinking of P. Hansma and coworkers (University of California, Santa Barbara) as to how calcified tissues resist fracture. Using a scanning probe spectroscopy setup with the ability to measure the force-elongation curve of single long chain molecules on the freshly fractured surface of biomineralized tissues[108-110], these researchers found that, when pulled, the organic molecules (which could be collagen[108] or other noncollageneous proteins[109, 110] show an initial relatively sharp increase of force with pulling length, followed by a long stretch with a characteristic series of drops and subsequent rises in force, as if a series of bonds internal to the molecule had yielded or broken. This typical force-elongation curve had thus a relatively large area under the curve, corresponding to high energy dissipation in the process of pulling the molecule, with minimal increase in force. It was further found that the amount of energy dissipation increased with the presence of calcium ions in the sample chamber where the pulling experiments were carried out. They also carried out high resolution electron microscopy measurements showing an amorphous, apparently organic, coating of material on and between freshly fractured fibril bundles and lamellae, Based on these observations, they proposed a model with noncollagenous proteins forming an amorphous "glue" layer between the mineralized collagen fibrils. The protein backbone of these molecules was proposed to be highly coiled and folded back on itself, with connections between different parts of the backbone formed by nonspecific, weak "sacrificial" bonds. The molecular level processes of irreversible deformation after bone yield were believed to be mainly in these glue molecules. Under stress, some "sacrificial" bonds inside these molecules would break and the folded up molecule would elongate, but the protein backbone itself would remain essentially unstretched. This mechanism enables a large increase in length (both of the molecule and of the tissue) with minimal increase in force, which means a highly energy absorbing or tough material.

To fully incorporate the idea of sacrificial bonds into what is currently known about bone mechanics, however, some apparently contradictory points must be reconciled. The main point is that the idea of a glue between fibrils which breaks and reforms bonds under external load would mean that even after stretching bone past the yield point and subsequently unloading, the stiffness of the bone would be the same (as the fibrils remain undamaged while there are presumably plenty of

sacrificial bonds left unbroken in the glue layer). However, this is not what is observed in bone, where after loading beyond the yield point and subsequent unloading, there is a clear reduction in stiffness observed (after correcting for viscoelastic effects), attributed to "microdamage" or "microcracks" formed during the post yield deformation. Secondly, as described below, it must be seen whether the fibrils themselves are indeed undamaged beyond yielding (as required by the model) or not. Finally, on a related note, while this is not a problem for the model as currently proposed, if the critical or load – limiting step in bone fracture is not the yielding within the noncollagenous glue layer but debonding between the mineral and collagen[111, 112], then noncollagenous proteins could indeed exist and have all the properties described in the model, but their deformation would not be the critical rate – limiting step in bone yielding and irreversible deformation.

Looking directly at the strain in the fibrils of bone as it is stretched, synchrotron small angle X-ray scattering combined with microtensile testing, on bovine fibrolamellar bone showed that the strain in the fibrils was always less than that and typically about 0.5 of the tissue strain as measured with video extensometry (Fig. 9, open squares)[104, 106]. Beyond the yield point, where the applied external stress results in minimal additional stress (low hardening) taken up, the fibril strain ε_F was observed to reach a constant value. Based on these two observations, Gupta *et al.*[104, 106] proposed a model of interfibrillar shearing, where the stiffer mineralized fibrils are loaded mainly in tension and the intervening extrafibrillar matrix is in shear. Such a model is effectively an 'equal stress' or Reuss model[113], where the large interfacial contact area between the fibril and the extrafibrillar matrix results in an effective load transfer despite the (presumably) weak and ductile nature of the extrafibrillar matrix. These results were correlated to the previous independent findings of an organic, "glue" like material between bone fibrils[104, 106], revealed using high resolution scanning electron microscopy. Such an organic glue, containing weak "sacrificial bonds" which may be opened under external force, was proposed to play a crucial role in the mechanics of bone[108, 109]. Interestingly, the fraction of strain taken up by the fibrils increased as the (bulk) elastic modulus increased[106], which could be explained by partial mineralization of the interfibrillar matrix, consistent with both structural observations[104, 106] and theoretical calculations[104, 106]. The constancy of the fibril strain beyond the yield point was attributed to a stick-slip mechanism where the fibrils decouple from the intrafibrillar matrix beyond a critical (yield) stress, at a strain of about 0.5 % in the fibril[104, 106].

The mineral crystallites are believed to have their c-axis parallel to the fibril. By doing both diffraction (on the mineral crystallographic lattice peaks) and small angle scattering (on the collagen axial periodicity) during micromechanical testing on bovine fibrolamellar bone (Fig. 9, open squares and closed circles), a hierarchical pattern of strain was seen in tension. 12 units of tissue strain translated to 5 units of strain on the fibril ε_F, which in turn transmitted only 2 units of strain to the mineral particles ε_M[104, 106]. While such a hierarchical staggered model[104, 106], shown schematically in Fig. 10, is a relatively simple and obvious design for a multi-scale composite, this construction enables the mismatch between the mechanical properties of the mineral (110 GPa[27, 104, 106]) and

collagen (1-2 GPa[104, 106, 114]) to work out for the benefit of the whole material. the mineral is loaded in tension via shearing stresses transmitted through the much softer collagen matrix. Bone mineral was also observed to be much stronger than bulk apatite[104, 106, 115], reaching strains of up to 0.3 %, which is quite large for a ceramic. This size effect is most probably because mineral platelets below a critical size (of the order of 30 nm[116]) can reach their theoretical strength (E/10 ~ 11 GPa for hydroxyapatite[113]), unaffected by flaws. While the maximum stress observed by Gupta *et al.*[105] = 0.3 % × 110 GPa = 3.3 GPa was lower than this value, it was also higher than the <1 GPa values expected from bulk apatite[104, 106]. On raising strain rates to physiological levels of ~0.2 s^{-1} (as compared to the 10^{-4} s^{-1} values used by Gupta *et al.*[104-106]) it is likely that the proportion of tissue strain taken up by the fibrils will increase, since the interfibrillar matrix is most likely highly viscous and would increase its effective stiffness with increasing strain rate.

Applying the same technique to the less mineralized but highly tough deer antler, as well as to *demineralised* fibrolamellar bone has revealed a more complex picture. Fibrils in antler initially stretch in linear proportion to the external tissue strain, with the same factor of 0.5 as in bone[117]. But following mechanical yielding fibrils do not stop at a constant strain level of 0.5 %, but there is increasing inter-fibrillar heterogeneity. Similar results are observed in EDTA-demineralised bone where the onset of fibrillar heterogeneity occurs around fibril strains of 0.5-1.0 %, although inter-sample variation does exist[118]. Similar to antler, the mean fibril strain continues to increase linearly. In contrast to bone and antler, demineralised bone matrix also shows some degree of fibrillar reorientation[118]-as expected for a more ductile material. In the collagen of demineralised bone, there is no transition from elastic to yielding behaviour, and two regimes of low stiffness (low strain “heel” part of the stress train curve) and a high modulus region (high strain linear part of the stress strain curve) are observed., as seen in to other collageneous tissues[119].

Bone and antler considered together show that, at the nanoscale, events associated with a transition to inelasticity manifest themselves as a form of interfibrillar sliding and decoupling. Depending on the degree of extra- and intrafibrillar mineralization, this could involve either (a) frictional sliding between extrafibrillar mineral platelets and elongation in the less mineralized collagen fibrils, or (b) sliding of mineralized collagen fibrils past each other (Fig. 11). Going beyond the general description of post yield deformation as due to some form of “damage” at the micron or sub-micron level[55, 120-123], it is clear that at the molecular level, such damage must correspond to the breakage of bonds and restructuring of material under load. Understanding the energetics of this bond breaking process was the focus of two recent works[124, 125], where the technique of thermal activation analysis was used to characterize the energy and volume characteristic of a basic unit irreversible deformation at the molecular level. The method treats the bond breakage as an Arrhenius-type rate process, in which the strain rate is proportional to $\exp(-H/k_BT)$. Application of external stress dramatically increases this rate, due to the work done by the applied stress over the deformation volume. Such a process can be

thus characterized by two parameters. *H*, an activation enthalpy and *v*, an activation volume. In this picture, the post yield stress level in bone can be reduced by reducing the strain rate ,as seen in Figure 12. By varying the testing conditions (temperature and strain rate) at which creep or tensile stretch to failure experiments[124] are done, the two parameters can be calculated to be $H \sim 1.1$ eV and $v \sim 0.65$ nm^3 (Fig. 13), suggesting that the weakest link in irreversible bone deformation is due to breakage of ionic bonds. This approach, while generally model free, does assume that strain rates as measured macroscopically are homogeneous over the micron level in the inelastic regime. Digital image correlation measurements of spatial distribution of tissue strains at the micron level[126] have shown that in bone, strong strain heterogeneities do occur in inelastic loading of bone. However, the experimental parameters are expected not to change significantly, due to their logarithmic dependence on strain rates[124]. Enhancement of strain rates by a factor of 3 in regions of highly strained tissue would change the activation volume by a factor of $\ln(3) = 1.1$ only.

Combining the synchrotron and the thermal activation analysis data, we suggest that beyond the yield point, mineralized collagen fibrils undergo some form of decohesion, either between fibrils or even inside a single fibril, during which ionic bonds are being broken (Fig. 14). Localized clusters of such breakage can grow and link up, as in conventional fibre composite materials[113], forming clusters which can be micron sized or larger and appear as 'damage' in confocal and light microscopy. Two candidates can be proposed for *where* this irreversible bond breakage occurs: the bonds between non-collagenous proteins and extrafibrillar mineral between fibrils (interfibrillar breakage)[104, 106, 124], or the bond between collagen and mineral within a fibril (mineral-collagen decohesion)[55].

Nonetheless, the fact that the fibril strain starts showing increased heterogeneity at fibril strain levels of 0.5-1.0 % even in *demineralised* bone is intriguing, and suggests that some structural property in the collagen matrix itself[127, 128] changes beyond the yield point in bone-although, again, we note that the macroscopic stress-strain curve of demineralised bone does not exhibit any discontinuity at this strain level. In this context, we note that Jäger[129] proposed a molecular level model of creep in organic materials, by considering the thermally assisted bond breaking of parallel arranged bonds. While the model is very general and not specific to bone or any other material, what is intriguing to us is that by applying the model to the published data of creep in (unmineralized) Wallaby tail tendons carried out by Wang and Ker[130-132], Jäger obtained an activation energy of 1.125 eV/atom, which is remarkably close to the 1.1 eV obtained by Gupta *et al.*[124] for (fully mineralized) bone. This could mean that the irreversible deformation and elongation is indeed occurring inside the collagen fibril, and not between fibrils, as originally proposed[104, 106].

4. Conclusions

To develop a clear picture of the structure/function relationships in bone, research follows two paths: (i) conventional material characterisation of its performance and (ii) structural

analysis of the mechanisms underlying bone fracture. For the latter, we can identify two main current challenges, one at the bone material level and one at the microstructural level. At the material level, one critical limitation now appears to be the difficulty in developing an accurate quantitative picture of the chemical nature of the bone mineral (amorphous or crystalline) and its distribution inside and around fibrils (clarifying the nanostructure). With such a structural picture, it would be possible to provide a clear model and interpretation of strain in different subphases of bone, and the onset of post yield deformation, which are now directly amenable to investigation using in-situ X-ray methods[104-106]. As of now, the models developed for bone deformation at the nanoscale must use (admittedly plausible) schemes of interfibrillar and intrafibrillar mineral packing in the collagen matrix obtained from complementary techniques like atomic force microscopy and electron microscopy[109, 133, 134]. The second challenge is, assuming a full understanding of bone 'matrix' properties, to develop computational schemes for predicting failure in both trabecular and compact bone at the microstructural and macrostructural level. The issue here is a more general materials engineering problem of the failure of partly regular cellular solids[135], and could be addressed with analytical, finite element and experimental methods. Experimentally, techniques like synchrotron microCT[136] and high speed photography can be very useful[137], in showing the onset of microcracking, damage etc. Such applications make it obvious that because of the spatial variations of bone properties, the mineral content and architecture in the microscale future analysis will be increasingly using modern microanalytical techniques to provide us with the answers we need.

Acknowledgments

P. Zioupos is grateful to various colleagues: R. Cook, K. Winwood, V. Wise, J.D. Currey, U. Hansen, A.J. Sedman, and also to J-Y. Rho whose untimely death was a great loss. H.S. Gupta would like to thank the Max Planck Society and the German-Israeli Foundation (Project No. I-800-180.10\2003) for support, and numerous coworkers, in particular: P. Fratzl, W. Wagermaier, S. Krauß, J. Seto, K. Kanawka, M. Kerschnitzki, G. Benecke, U. Stachewicz, and P. Roschger.

Figures

Fig. 1. (a) Consecutive stages of behaviour: the elastic range (E), the continuum damage mechanics range (CDM), and the fracture mechanics (FM) one[2]. Unfortunately mechanical material tests of bone each concentrate on one of these domains with little overlap across them and therefore fail to apply a holistic approach to the problem. The relative length (or time spent) on any of the 3 regions can vary widely depending on specimen geometry, the applied loading protocol and other conditions, hence a wide variety of stress/strain recordings may result. (b) During fracture, energy is dissipated/absorbed

in a number of ways, either elastically, or as prefailure damage (microcracks), or in growing a slow moving crack with its collateral damage, or into advancing a fast moving fracture plane.

Fig. 2. (a) Fracture toughness (initiation) values in human cortical bone in SENB samples with age with the crack in the transverse to the grain direction[17] (bone sector as symbols: A.anterior, P.posterior, L.lateral). (b) Initiation and growth fracture toughness values with age and crack length redrawn from Nalla *et al.*[14, 15].

Fig. 3. Crack propagation: (a) The energy required to propagate a crack in the radial (m: microcracking damage), tangential (d: deflected crack) and circumferential (b: brittle fracture) directions in bovine bone with the crack length. Bone is much tougher in the fracture mode accompanied by microcracking damage (m) ahead of it[2, 4]. (b) The energy required to drive a crack across the grain (fibre direction) is an order of magnitude higher than along it[4].

Fig. 4. (a) Work of fracture (slow and controllable mode tests) vs. Impact energy absorption in specimens of human cortical bone of various ages ranging from 4 to 82 yrs old (age as symbol; R^2=0.69). There is a correlation between the two measures, which shows that the underlying cause is the ageing process itself, not the way in which the fracture is quantified[19]. (b) W_f as a function of the stroke rate during the test in 4 bone types: human (unpublished data provided by PZ), tiger, and bovine femurs; and deer antler material[2]. With the exception of antler, the three 'normal' bones experience a ductile-to-brittle transition for stroke rates above 5 mm/min (strain rate: 1.5×10^{-3} s^{-1}). The percentage numbers show what fraction of the specimens achieved a ductile fracture.

Fig. 5. Ductile-to-brittle transition observed in human femoral bone in tension (single pulls to failure, the critical strain rate, for a 10 mm gauge length, is 0.01-0.1 s^{-1}). Above the strain rate threshold the post-yield region, the capacity for energy absorption, and the microcracking damage reduce significantly[18, 140].

Fig. 6. The growth of cracks is strongly influenced by the structure[39] as shown when the separate and added effects of (i) microstructural heterogeneity and (ii) physical characteristics were examined in the fatigue strength of cortical bone in 3 modes .tension, compression and shear. The photo shows a large surface crack which emanated laterally from the fracture surface (on the right of the photo) and grew towards the left advancing naturally between the various bone compartments along boundaries on either side of which the composition and architecture changed sharply.

Fig. 7. Lamellar level modulation of mechanics and fiber orientation in bone osteons (Haversian systems) (a) Indentation modulus (stiffness), mapped with 1 μm steps along the radius of an osteon from the femur of a woman shows periodic variations from 24-27 GPa[41]. Scanning electron microscopy image of a typical osteon is shown on the right, with the dashed rectangle indicating the usual width of radial sector used to generate a modulus map. (b) Fibril orientation relative to long axis shows a plywood like[58] radial periodic variation (dashed rectangle), as quantified by scanning microtexture experiments[68, 69]. On average, fibrils are here observed to spiral in a

right handed manner around the central blood vessel. On the right, a polarized light microscope image of a typical osteon shows (dashed rectangle) the usual size of the radial sector in which the scans were done. Best fit solid lines (sinusoidal in (a) and exponentially damped sinusoidal in (b)) are meant as guides to the eye.

Fig. 8. (a) Schematic view of in-situ tensile testing of bone in the synchrotron [104-106]. High intensity X-ray radiation is used to generate small-angle (SAXS) and wide-angle (WAXD) images of bone nanostructure, concurrently with mechanical deformation. (b) Integrated intensity plots I(q) can quantify fibrillar & mineral structure. On the right, a typical variation of collagen fibril periodicity (D) and width of the meridional reflection (SD) with applied tissue strain is shown.

Fig. 9. (a) Fibril (squares) and mineral (circles) strain response to applied tissue strain using in-situ tensile testing with synchrotron diffraction. N=21, error bars are standard deviations. Initial response of fibril and mineral strain is linear, but nonlinearity and plateau behaviour is observed beyond the yield point. Line of equal strains given by dash-dotted line. Data from Gupta *et al.*[105].

Fig. 10. Tensile strain in bone is transferred in successively lower fractions from the tissue to the nanoscale level on applied external load[105]. Shearing in the intervening soft phase accommodates the remaining strain at each level: in the interfibrillar matrix at the fibril level and in the collagen matrix at the mineral platelet level.

Fig. 11. Two possible schemes for the post yield behaviour at the nanoscale level, which may be different across tissue types and degrees of mineralization: (1) fibrils continue to stretch, possibly heterogeneously, and decouple from the (extrafibrillar) mineral. (2) Mineralized fibrils decouple and slide past each other, and maintain a constant level of fibril strain.

Fig. 12. Strain-rate sensitivity of the post yield behaviour of bone. Reducing the stretching velocity from 10 $\mu m\ s^{-1}$ to 0.5 $\mu m\ s^{-1}$ results in a ~ 10 MPa drop in stress[124]; inset shows that the linear hardening slopes at the different strain rates (shown schematically by the dashed lines) are approximately the same.

Fig. 13. (a) Two dimensional view of the variation of yield stress σ_Y with temperature and applied strain rate, showing decrease of σ_Y with increasing temperature and decreasing strain rate. N = 63 samples are shown here. (b) One-dimensional view of the same set of data, averaged over each (temperature, strain rate) pair. Data from Fig. 3 in Gupta *et al.*[124].

Fig. 14. Schematic of ionic bond breaking in interfibrillar matrix of bone, between negatively charged polyelectrolyte molecules like osteopontin and divalent ions like calcium[124].

Table 1. List of methods for determining the elastic modulus of trabecular bone material and the resulting estimate values. Modified from the original in Rho *et al.*[1].

Reference	*Test Method*	*Estimate of elastic modulus (GPa)*
Wolff [78]	Hypothesis	17-20 (assumption)
Runkle and Pugh [79]	Buckling	8.69±3.17 (dry)
Townsend *et al.* [80]	Inelastic buckling	11.38 (wet)
Williams and Lewis [81]	Back-calculation from FEA	1.30
Ashman and Rho [38]	Ultrasound test method	12.7±2.0 (wet)
Ryan and Williams [85]	Tensile testing	0.76±0.39
Hodgskinson *et al.* [82]	Microhardness	15 (estimation)
Kuhn *et al.* [83]	Three-point bending	3.81 (wet)
Mente and Lewis [84]	Cantilever bending with FEA	7.8±5.4 (dry)
Choi *et al.* [35]	Four-point bending	5.35±1.36 (wet)
	Tensile testing	10.4±3.5 (dry)
Rho *et al.* [76]	Ultrasound test method	14.8±1.4 (wet)
Rho *et al.* [66]	Nanoindentation	19.6±3.5 (along); 15.0±3.0 (across)
Bini et al. [138]	Microtensile tests	1-2
Coats *et al.* [139]	Microhardness	9-11

References.

1. J. Y. Rho, L. Kuhn-Spearing and P. Zioupos. Mechanical properties and the hierarchical structure of bone. Medical Engineering & Physics 1998; 20:92-102.
2. P. Zioupos. Recent developments in the study of failure of solid biomaterials and bone. `fracture' and `pre-fracture' toughness. Materials Science & Engineering C:Biomimetic Materials, Sensors & Systems 1998; C6:33-40.
3. K. Piekarski. Fractography of bone. In: G. W. Hastings and P. Ducheyne, editor. Natural and Living Biomaterials. Boca Raton, Floriú. CRC Press Inc., 1984.
4. H. Peterlik, P. Roschger, K. Klaushofer and P. Fratzl. From brittle to ductile fracture of bone. Nature Materials 2006; 5:52-55.
5. A. P. Jackson, J. F. V. Vincent and R. M. Turner. A Physical Model of Nacre. Composites Science and Technology 1989; 36:255-266.
6. R. Z. Wang, H. B. Wen, F. Z. Cui, H. B. Zhang and H. D. Li. Observations of damage morphologies in nacre during deformation and fracture. Journal of Materials Science 1995; 30:2299-2304.
7. D. M. Robertson, D. Robertson and C. R. Barrett. Fracture toughness, critical crack length and plastic zone size in bone. J. Biomech. 1978; 11:359-364.
8. J. W. Melvin. Fracture mechanics of bone. J.Biomech.Eng/Trans ASME 1993; 115:549-554.
9. K. J. Koester, J. W. Ager and R. O. Ritchie. The true toughness of human cortical bone measured with realistically short cracks. Nature Materials 2008; 7:672-677.
10. D. Vashishth, J.C. Behiri, K.E. Tanner and W. Bonfield, Toughening mechanisms in cortical bone, 42nd Ann. Meeting ORS, Feb.19-22, 1996, Atlanta, Georgia, USA.
11. J. J. Kruzic, J. A. Scott, R. K. Nalla and R. O. Ritchie. Propagation of surface fatigue cracks in human cortical bone. Journal of Biomechanics 2006; 39:968-972.
12. R. K. Nalla, J. S. Stolken, J. H. Kinney and R. O. Ritchie. Fracture in human cortical bone. local fracture criteria and toughening mechanisms. Journal of Biomechanics 2005; 38:1517-1525.
13. R. O. Ritchie, J. H. Kinney, J. J. Kruzic and R. K. Nalla. A fracture mechanics and mechanistic approach to the failure of cortical bone. Fatigue & Fracture of Engineering Materials & Structures 2005; 28:345-371.
14. R. K. Nalla, J. J. Kruzic, J. H. Kinney and R. O. Ritchie. Mechanistic aspects of fracture and R-curve behavior in human cortical bone. Biomaterials 2005; 26:217-231.
15. R. K. Nalla, J. J. Kruzic, J. H. Kinney and R. O. Ritchie. Effect of aging on the toughness of human cortical bone: evaluation by R-curves. Bone 2004; 35:1240-1246.
16. R. K. Nalla, J. H. Kinney and R. O. Ritchie. Mechanistic fracture criteria for the failure of human cortical bone. Nature Materials 2003; 2:164-168.
17. P. Zioupos and J. D. Currey. Changes in the stiffness, strength, and toughness of human cortical bone with age. Bone 1998; 22:57-66.

18. U. Hansen, P. Zioupos, R. Simpson, J. D. Currey and D. Hynd. The effect of strain rate on the mechanical properties of human cortical bone. J.Biomech.Eng/Trans ASME 2008; 130:011011-18.
19. J. D. Currey, K. Brear and P. Zioupos. The effects of ageing and changes in mineral content in degrading the toughness of human femora. Journal of Biomechanics 1996; 29:257-260.
20. J. D. Currey. Tensile yield in compact bone is determined by strain, post-yield behaviour by mineral content. Journal of Biomechanics 2004; 37:549-556.
21. J. D. Currey, K. Brear and P. Zioupos. Notch sensitivity of mineralised tissues in impact. Proceedings of the Royal Society of London Series B-Biological Sciences 2004; 271:517-522.
22. P. Zioupos and J. D. Currey. The Extent of Microcracking and the Morphology of Microcracks in Damaged Bone. Journal of Materials Science 1994; 29:978-986.
23. P. Zioupos, J. D. Currey and A. J. Sedman. An Examination of the Micromechanics of Failure of Bone and Antler by Acoustic-Emission Tests and Laser-Scanning-Confocal-Microscopy. Medical Engineering & Physics 1994; 16:203-212.
24. P. Zioupos and J. D. Currey. Pre-failure toughening mechanisms in the dentine of the narwhal tusk. Microscopic examination of stress/strain induced microcracking. Journal of Materials Science Letters 1996; 15:991-994.
25. P. Zioupos, X. T. Wang and J. D. Currey. Experimental and theoretical quantification of the development of damage in fatigue tests of bone and antler. Journal of Biomechanics 1996; 29:989-1002.
26. P. Zioupos, X. T. Wang and J. D. Currey. The accumulation of fatigue microdamage in human cortical bone of two different ages in vitro. Clinical Biomechanics 1996; 11:365-375.
27. S. Weiner and H. D. Wagner. The material bone. Structure mechanical function relations. Annu. Rev. Mater. Sci. 1998; 28:271-298.
28. D. R. Carter and W. Hayes. The compressive behavior of bone as a two-phase porous structure. Journal of Bone and Joint Surgery 1977; 59A:954-962.
29. L. J. Gibson. The mechanical behavior of cancellous bone. Journal of Biomechanics 1985; 18:317-328.
30. D. H. Enlow. Principles of bone remodeling. Charles C Thomas, Springfield, IL, 1963.
31. D. H. Enlow. The human face. An account of the postnatal growth and development of the craniofacial skeleton. Harper and Row, New York, 1968.
32. T. S. Keller, Z. Mao and D. M. Spengler. Young's Modulus, Bending Strength, and Tissue Physical-Properties of Human Compact-Bone. Journal of Orthopaedic Research 1990; 8:592-603.
33. D. R. Carter, G. H. Schwab and D. M. Spengler. Tensile Fracture of Cancellous Bone. Acta Orthopaedica Scandinavica 1980; 51:733-741.
34. P. Zioupos, C. Kaffy and J. D. Currey. Tissue heterogeneity, composite architecture and fractal

dimension effects in the fracture of ageing human bone. International Journal of Fracture 2006; 139:407-424.

35. K. Choi, J. L. Kuhn, M. J. Ciarelli and S. A. Goldstein. The Elastic-Moduli of Human Subchondral, Trabecular, and Cortical Bone Tissue and the Size-Dependency of Cortical Bone Modulus. Journal of Biomechanics 1990; 23:1103-1113.
36. K. W. Choi and S. A. Goldstein. The fatigues properties of bone tissues on a microstructural level. In. editor. City. 1991.
37. J. C. Rice, S. C. Cowin and J. A. Bowman. On the Dependence of the Elasticity and Strength of Cancellous Bone on Apparent Density. Journal of Biomechanics 1988; 21:155-168.
38. R. B. Ashman and J. Y. Rho. Elastic-Modulus of Trabecular Bone Material. Journal of Biomechanics 1988; 21:177-181.
39. P. Zioupos, M. Gresle and K. Winwood. Fatigue strength of human cortical bone: age, physical and material heterogeneity effects. Journal of Biomedical Materials Research 2008; 86:627–636.
40. C. H. Turner, J. Rho, Y. Takano, T. Y. Tsui and G. M. Pharr. The elastic properties of trabecular and cortical bone tissues are similar: results from two microscopic measurement techniques. Journal of Biomechanics 1999; 32:437-441.
41. H. S. Gupta, U. Stachewicz, W. Wagermaier, P. Roschger, H. D. Wagner and P. Fratzl. Mechanical Modulation at the Lamellar Level in Osteonal Bone. Journal of Materials Research 2006; 21:1913-1921.
42. J. Juist. In vivo determination of the elastic response of bone-2: Ulnar resonant frequency in osteoporotic, diabetic and normal subjects. Physics in Medicine and Biology 1970; 15.427-434.
43. A. B. Christensen, F. Ammitzboll, C. Dyrbye, M. Cornelissen, P. Cornelissen and G. Vanderperre. Assessment of Tibial Stiffness by Vibration Testing In-situ-1: Identification of Mode Shapes in Different Supporting Conditions. Journal of Biomechanics 1986; 19:53-60.
44. J. Y. Rho, M. C. Hobatho and R. B. Ashman. Relations of Mechanical-Properties to Density and CT Numbers in Human Bone. Medical Engineering & Physics 1995; 17:347-355.
45. S. Goldstein. The mechanical properties of trabecular bone. dependence on anatomic location and function. Journal of Biomechanics 1987; 20:1055-1061.
46. B. VanRietbergen, A. Odgaard, J. Kabel and R. Huiskes. Direct mechanics assessment of elastic symmetries and properties of trabecular bone architecture. Journal of Biomechanics 1996; 29:1653-1657.
47. A. Odgaard, J. Kabel, B. VanRietbergen, M. Dalstra and R. Huiskes. Fabric and elastic principal directions of cancellous bone are closely related. Journal of Biomechanics 1997; 30:487-495.
48. F. Linde and I. Hvid. The effect of constraint on the mechanical behaviour of trabecular bone specimens. Journal of Biomechanics 1989; 22:485-490.
49. A. Odgaard and F. Linde. The underestimation of Young modulus in compressive testing of

cancellous bone specimens. Journal of Biomechanics 1991; 24:691-698.
50. T. M. Keaveny, T. P. Pinilla, R. P. Crawford, D. L. Kopperdahl and A. Lou. Systematic and random errors in compression testing of trabecular bone. Journal of Orthopaedic Research 1997; 15:101-110.
51. A. Ascenzi and E. Bonucci. The tensile properties of single osteons. Anatomical Record 1967; 158:375-386.
52. A. Ascenzi and E. Bonucci. The compressive properties of single osteons. Anatomical Record 1968; 161:377-392.
53. A. Ascenzi and E. Bonucci. The bending properties of single osteons. Journal of Biomechanics 1990; 23:763-771.
54. A. Ascenzi, P. Baschieri and A. Benvenuti. The Torsional Properties of Single Selected Osteons. Journal of Biomechanics 1994; 27:875-&.
55. C. Mercer, M. Y. He, R. Wang and A. G. Evans. Mechanisms governing the inelastic deformation of cortical bone and application to trabecular bone. Acta Biomater. 2006; 2:59-68.
56. G. Marotti. A new theory of bone lamellation. Calcified Tissue International 1993; 53.S47-S56.
57. S. Weiner, W. Traub and H. D. Wagner. Lamellar bone. Structure-function relations. Journal of Structural Biology 1999; 126:241-255.
58. M. M. Giraud-Guille. Twisted Plywood Architecture of Collagen Fibrils in Human Compact-Bone Osteons. Calcified Tissue International 1988; 42:167-180.
59. S. Weiner, T. Arad, I. Sabanay and W. Traub. Rotated plywood structure of primary lamellar bone in the rat: Orientations of the collagen fibril arrays. Bone 1997; 20:509-514.
60. S. Weiner and W. Traub. Bone-Structure-from Angstroms to Microns. Faseb J. 1992; 6:879-885.
61. M. M. Giraud-Guille. Cholesteric Twist of Collagen In vivo and In vitro: Molecular Crystals and Liquid Crystals 1987; 153:15-30.
62. P. Frasca, R. A. Harper and J. L. Katz. Collagen fiber orientations in human secondary osteons. Acta Anatomica 1977; 98:1-13.
63. K. Hasegawa, C. H. Turner and D. B. Burr. Contribution of Collagen and Mineral to the Elastic-Anisotropy of Bone. Calcified Tissue International 1994; 55:381-386.
64. C. H. Turner and D. B. Burr. Orientation of collagen in osteonal bone. Calcified Tissue International 1997; 60:90.
65. R. M. Pidaparti, A. Chandran, T. Y. and C. H. Turner. Bone mineral lies mainly outside of collagen fibrils. predictions of a composite model for osteonal bone. Journal of Biomechanics 1996; 29:909-916.
66. J. Y. Rho, M. Roy, T. Y. Tsui and G. M. Pharr. Young's modulus and hardness of trabecular and cortical bone in various directions determined by nanoindentation. Tran. 43th Annual Meetings Orthop. Res. Soc., San Francisco, CA, 1997, 891.
67. G. Willems, J. P. Celis, P. Lambrechts, M. Braem and G. Vanherle. Hardness and Young's

modulus determined by nanoindentation technique of filler particles of dental restorative materials compared with human enamel. Journal of Biomedical Materials Research 1993; 27:747-755.

68. W. Wagermaier, H. S. Gupta, A. Gourrier, O. Paris, P. Roschger, M. Burghammer, C. Riekel and P. Fratzl. Scanning texture analysis of lamellar bone using microbeam synchrotron X-ray radiation. Journal of Applied Crystallography 2007; 40:115-120.
69. W. Wagermaier, H. S. Gupta, A. Gourrier, M. Burghammer, P. Roschger and P. Fratzl. Spiral twisting of fiber orientation inside bone lamellae. Biointerphases 2006; 1:1-5.
70. J. Y. Rho, J. D. Currey, P. Zioupos and G. M. Pharr. The anisotropic Young's modulus of equine secondary osteones and interstitial bone determined by nanoindentation. Journal of Experimental Biology 2001; 204:1775-1781.
71. J. Xu, J. Y. Rho, S. R. Mishra and Z. Fan. Atomic force microscopy and nanoindentation characterization of human lamellar bone prepared by microtome sectioning and mechanical polishing technique. Journal of Biomedical Materials Research Part A 2003; 67A:719-726.
72. J. Y. Rho, S. R. Mishra, K. Chung, J. Bai and G. M. Pharr. Relationship between ultrastructure and the nanoindentation properties of intramuscular herring bones. Annals of Biomedical Engineering 2001; 29:1082-1088.
73. P. Fratzl, H. S. Gupta, E. P. Paschalis and P. Roschger. Structure and mechanical quality of the collagen-mineral nano-composite in bone. J. Mater. Chem. 2004; 14:2115-2123.
74. R. Lakes and S. Saha. Cement Line Motion in Bone. Science 1979; 204:501-503.
75. J. L. Katz and A. Meunier. Scanning Acoustic Microscope Studies of the Elastic Properties of Osteons and Osteon Lamallae. J.Biomech.Eng/Trans ASME 1993; 115:543-548.
76. J. Y. Rho, R. B. Ashman and C. H. Turner. Youngs Modulus of Trabecular and Cortical Bone Material-Ultrasonic and Microtensile Measurements. Journal of Biomechanics 1993; 26:111-119.
77. D. T. Reilly, A. H. Burstein and V. H. Frankel. Elastic-Modulus for Bone. Journal of Biomechanics 1974; 7:271-&.
78. J. Wolff. Das Gesetz der Transformation der Knochen. Hirschwald, Berlin, 1892.
79. J. C. Runkle and J. Pugh. The micro-mechanics of cancellous bone. Bulletin of Hospital Joint Diseases 1975; 36:2-10.
80. P. R. Townsend, R. M. Rose and E. L. Radin. Buckling studies of single human trabeculae. Journal of Biomechanics 1975; 8:199-201.
81. J. L. Williams and J. L. Lewis. Properties and an anisotropic model of cancellous bone from the proximal tibial epiphysis. J.Biomech.Eng/Trans ASME 1982; 104:50-56.
82. R. Hodgkinston, J. D. Currey and G. P. Evans. Hardness, an indicator of the mechanical competence of cancellous bone. Journal of Orthopaedic Research 1989; 7:754-758.
83. J. L. Kuhn, S. A. Goldstein, K. W. Choi, M. London, L. A. Feldkamp and L. S. Matthews.

Comparison of the trabecular and cortical tissue moduli from human iliac crests. Journal of Orthopaedic Research 1989; 7:876-884.

84. P. L. Mente and J. L. Lewis. Experimental method for the measurement of the elastic modulus of trabecular bone tissue. Journal of Orthopaedic Research 1989; 7:456-461.
85. C. B. Ryan and J. L. Williams. Tensile testing of rodlike trabeculae excised from bovine femoral bone. Journal of Biomechanics 1989; 22:351-355.
86. M. J. Glimcher. Mechanisms of calcification. role of collagen fibrils and collagen-phsophoprotein complexes in vitro and in vivo. Anatomical Record 1989; 224:139-153.
87. L. Kuhn-Spearing, C. Rey, H. M. Kim and M. J. Glimcher. Carbonated apatite nanocrystals of bone. In. D. L. Bourell (editor) Synthesis and processing of nanocrystalline powder. Warrendale, PA, USA. The Minerals, Metals and Materials Society, 1996.
88. W. J. Landis. The strength of a calcified tissue depends in part on the molecular structure and organization of its constituent mineral crystals in their organic matrix. Bone 1995; 16:533-544.
89. V. Ziv and S. Weiner. Bone crystal size: a comparison of transmission electron microscopic and x-ray diffraction line-width-broadening techniques. Connective Tissue Research 1994; 30:165-175.
90. J. Sodek, B. Ganss and M. D. McKee. Osteopontin: Critical Reviews in Oral Biology & Medicine 2000; 11:279-303.
91. M. D. McKee and A. Nanci. Osteopontin at mineralized tissue interfaces in bone, teeth, and osseointegrated implants: Ultrastructural distribution and implications for mineralized tissue formation, turnover, and repair. Microscopy Research and Technique 1996; 33:141-164.
92. M. F. Young, J. M. Kerr, K. Ibaraki, A. M. Heegaard and P. G. Robey. Structure, expression, and regulation of the major noncollagenous matrix proteins of bone. Clinical Orthopaedics and Related Research 1992; 275-294.
93. P. V. Hauschka, J. B. Lian, D. E. C. Cole and C. M. Gundberg. Osteocalcin and matrix GLA protein-Vitamin K dependent proteins in bone. Physiological Reviews 1989; 69:990-1047.
94. L. C. Bonar, S. Lees and H. A. Mook. Neutron-Diffraction Studies of Collagen in Fully Mineralized Bone. Journal of Molecular Biology 1985; 181:265-270.
95. S. Lees, N. J. Tao and S. M. Lindsay. Studies of compact hard tissues and collagen by means of Brillouin light scattering. Connective Tissue Research 1990; 24:187-205.
96. S. Lees. Mineralization of type-I collagen. Biophysical Journal 2003; 85:204-207.
97. W. J. Landis, K. J. Hodgens, J. Arena, M. J. Song and B. F. McEwen. Structural relations between collagen and mineral in bone as determined by high voltage electron microscopic tomography. Microscopy Research and Technique 1996; 33:192-202.
98. W. J. Landis, K. J. Hodgens, M. J. Song, J. Arena, S. Kiyonaga, M. Marko, C. Owen and B. F. McEwen. Mineralization of collagen may occur on fibril surfaces. evidence from conventional and high-voltage electron microscopy and three-dimensional imaging. J. Struct. Biol. 1996;

117:24.

99. M. A. Rubin, L. Jasiuk, J. Taylor, J. Rubin, T. Ganey and R. P. Apkarian. TEM analysis of the nanostructure of normal and osteoporotic human trabecular bone. Bone 2003; 33:270-282.
100. M. J. Glimcher. The nature of the mineral component of bone and the mechanism of calcification. 1987; 49-69.
101. S. Weiner and W. Traub. Crystal Size and Organization in Bone. Connective Tissue Research 1989; 21:589-595.
102. S. Weiner, T. Arad and W. Traub. Crystal Organization in Rat Bone Lamellae. Febs Letters 1991; 285:49-54.
103. J. Y. Rho, T. Y. Tsui and G. M. Pharr. Elastic properties of human cortical and trabecular lamellar bone measured by nanoindentation. Biomaterials 1997; 18:1325-1330.
104. H. S. Gupta, W. Wagermaier, G. A. Zickler, J. Hartmann, S. S. Funari, P. Roschger, H. D. Wagner and P. Fratzl. Fibrillar level fracture in bone beyond the yield point. International Journal of Fracture 2006; 139:425-436.
105. H. S. Gupta, J. Seto, W. Wagermaier, P. Zaslansky, P. Boesecke and P. Fratzl. Cooperative deformation of mineral and collagen in bone at the nanoscale. Proceedings of the National Academy of Sciences of the United States of America 2006; 103:17741-17746.
106. H. S. Gupta, W. Wagermaier, G. A. Zickler, D. R. B. Aroush, S. S. Funari, P. Roschger, H. D. Wagner and P. Fratzl. Nanoscale deformation mechanisms in bone. Nano Letters 2005; 5:2108-2111.
107. J. D. Almer and S. R. Stock. Internal strains and stresses measured in cortical bone via high-energy X-ray diffraction. Journal of Structural Biology 2005; 152:14-27.
108. J. B. Thompson, J. H. Kindt, B. Drake, H. G. Hansma, D. E. Morse and P. K. Hansma. Bone indentation recovery time correlates with bond reforming time. Nature 2001; 414:773-776.
109. G. Fantner, T. Hassenkam, J. H. Kindt, J. C. Weaver, H. Birkedal, L. Pechenik, J. A. Cutroni, G. A. G. Cidade, G. D. Stucky, D. E. Morse and P. K. Hansma. Sacrificial bonds and hidden length dissipate energy as mineralized fibrils separate during bone fracture. Nature Materials 2005; 4:612-616.
110. P. K. Hansma, G. E. Fantner, J. H. Kindt, P. J. Thurner, G. Schitter, S. F. Udwin and M. M. Finch. Sacrificial bonds in the interfibrillar matrix of bone. J. Musculoskelet. Neuron. Interact. 2005; 5:313-315.
111. K. Tai, F. J. Ulm and C. Ortiz. Nanogranular origins of the strength of bone. Nano Lett. 2006; 6:2520-2525.
112. K. Tai, M. Dao, S. Suresh, A. Palazoglu and C. Ortiz. Nanoscale heterogeneity promotes energy dissipation in bone. Nature Materials 2007; 6:454-462.
113. D. Hull and T. W. Clyne. An introduction to composite materials, 2nd edition, Cambridge University Press, Cambridge, UK, 1996.

114. S. A. Wainwright, Biggs, W.D., Currey, J.D., Gosline, J.M.. Mechanical Design in Organisms. Princeton University Press, 1982.
115. A. J. Ruys, M. Wei, C. C. Sorrell, M. R. Dickson, A. Brandwood and B. K. Milthorpe. Sintering Effects on the Strength of Hydroxyapatite. Biomaterials 1995; 16:409-415.
116. H. J. Gao, B. H. Ji, I. L. Jäger, E. Arzt and P. Fratzl. Materials become insensitive to flaws at nanoscale: Lessons from nature. Proceedings of the National Academy of Sciences of the United States of America 2003; 100:5597-5600.
117. H. S. Gupta, S. Krauß, K. Kanawka, A. Gourrier, J. Seto, S. S. Funari, S. V. Roth, J. D. Currey, T. Landete-Castillejos, M. Rousseau and P. Fratzl. Mechanical and structural characterization of antler and nacre using small angle X-ray scattering. HASYLAB Annual Report 2006, 1169-1170.
118. K. Kanawka, Master of Science, Ultrastructural deformation in the fibrillar matrix of demineralized bone, Biomaterials Department, Max Planck Institute of Colloids and Interfaces and Fachhochschule Muenster, Potsdam, Germany, 2006.
119. J. Kastelic and E. Baer. Deformation in tendon collagen. Symposia of the Society for Experimental Biology 1980; 34:397-435.
120. D. Taylor, J. G. Hazenberg and T. C. Lee. Living with cracks. Damage and repair in human bone. Nature Materials 2007; 6:263-268.
121. T. Diab, K. W. Condon, D. B. Burr and D. Vashishth. Age-related change in the damage morphology of human cortical bone and its role in bone fragility. Bone 2006; 38:427-431.
122. T. L. A. Moore and L. J. Gibson. Microdamage accumulation in bovine trabecular bone in uniaxial compression. J.Biomech.Eng/Trans ASME 2002; 124:63-71.
123. G. C. Reilly and J. D. Currey. The effects of damage and microcracking on the impact strength of bone. Journal of Biomechanics 2000; 33:337-343.
124. H. S. Gupta, P. Fratzl, M. Kerschnitzki, G. Benecke, W. Wagermaier and H. O. K. Kirchner. Evidence for an elementary process in bone plasticity with an activation enthalpy of 1 eV. Journal of the Royal Society Interface 2007; 4:277-282.
125. H. Kirchner. Ductility and brittleness of bone. International Journal of Fracture 2006; 139:509-516.
126. G. Benecke, M. Kerschnitki, P. Fratzl and H. S. Gupta. Digital image correlation shows localized deformation bands in inelastic loading of fibrolamellar bone (In preparation, 2008).
127. P. Zioupos. Ageing human bone. Factors affecting its biomechanical properties and the role of collagen. J. Biomater. Appl. 2001; 15:187-229.
128. P. Zioupos, J. D. Currey and A. J. Hamer. The role of collagen in the declining mechanical properties of aging human cortical bone. Journal of Biomedical Materials Research 1999; 45:108-116.
129. I. L. Jäger. A model for the stability and creep of organic materials. Journal of Biomechanics

2005; 38:1459-1467.

130. X. T. Wang and R. F. Ker. Creep-Rupture of Wallaby Tail Tendons. Journal of Experimental Biology 1995; 198:831-845.
131. X. T. Wang, R. F. Ker and R. M. Alexander. Fatigue Rupture of Wallaby Tail Tendons. Journal of Experimental Biology 1995; 198:847-852.
132. R. F. Ker and P. Zioupos. Creep and Fatigue damage of mammalian tendon and bone. Comments in Theoretical Biology 1997; 4:151-81.
133. T. Hassenkam, G. E. Fantner, J. A. Cutroni, J. C. Weaver, D. E. Morse and P. K. Hansma. High-resolution AFM imaging of intact and fractured trabecular bone. Bone 2004; 35:4-10.
134. M. A. Rubin, J. Rubin and W. Jasiuk. SEM and TEM study of the hierarchical structure of C57BL/6J and C3H/HeJ mice trabecular bone. Bone 2004; 35:11-20.
135. L. J. Gibson. Cellular solids. MRS Bulletin 2003; 28:270-271.
136. P. J. Thurner, P. Wyss, R. Voide, M. Stauber, M. Stampanoni, U. Sennhauser and R. Müller. Time-lapsed investigation of three-dimensional failure and damage accumulation in trabecular bone using synchrotron light. Bone 2006; 39:289-299.
137. P. J. Thurner, B. Erickson, Z. Schriock, J. Langan, J. Scott, M. Zhao, J. C. Weaver, G. E. Fantner, P. Turner, J. H. Kindt, G. Schitter, D. E. Morse and P. K. Hansma. High-speed photography of the development of microdamage in trabecular bone during compression. Journal of Materials Research 2006; 21:1093-1100.
138. F. Bini, A. Marinozzi, F. Marinozzi and F. Patane. Microtensile measurements of single trabeculae stiffness in human femur. Journal of Biomechanics 2002; 35:1515-1519.
139. A. M. Coats, P. Zioupos and R. M. Aspden. Material properties of subchondral bone from patients with osteoporosis or osteoarthritis by microindentation testing and electron probe microanalysis. Calcified Tissue International 2003; 73:66-71.
140. P. Zioupos, U. Hansen, J.D. Currey. Microcracking damage and the fracture process in relation to strain rate in human cortical bone tensile failure. J Biomechanics 2008; In Press.

Figures

Fig. 1. (a) Consecutive stages of behaviour: the elastic range (E), the continuum damage mechanics range (CDM), and the fracture mechanics (FM) one[2]. Unfortunately mechanical material tests of bone each concentrate on one of these domains with little overlap across them and therefore fail to apply a holistic approach to the problem. The relative length (or time spent) on any of the 3 regions can vary widely depending on specimen geometry, the applied loading protocol and other conditions, hence a wide variety of stress/strain recordings may result. (b) During fracture, energy is dissipated/absorbed in a number of ways, either elastically, or as prefailure damage (microcracks), or in growing a slow moving crack with its collateral damage, or into advancing a fast moving fracture plane.

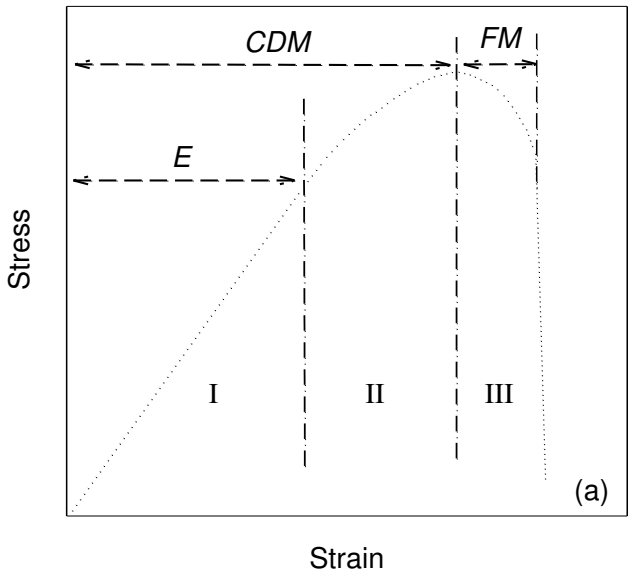

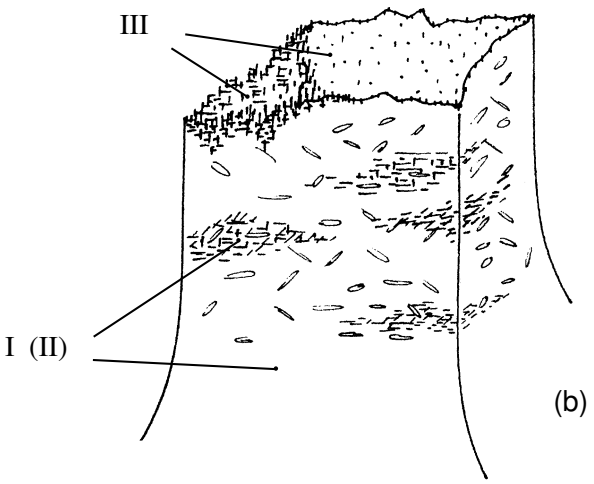

Fig. 2. (a) Fracture toughness (initiation) values in human cortical bone in SENB samples with age with the crack in the transverse to the grain direction[16] (bone sector as symbols: A:anterior, P:posterior, L:lateral). (b) Initiation and growth fracture toughness values with age and crack length redrawn from Nalla *et al.*[13, 14].

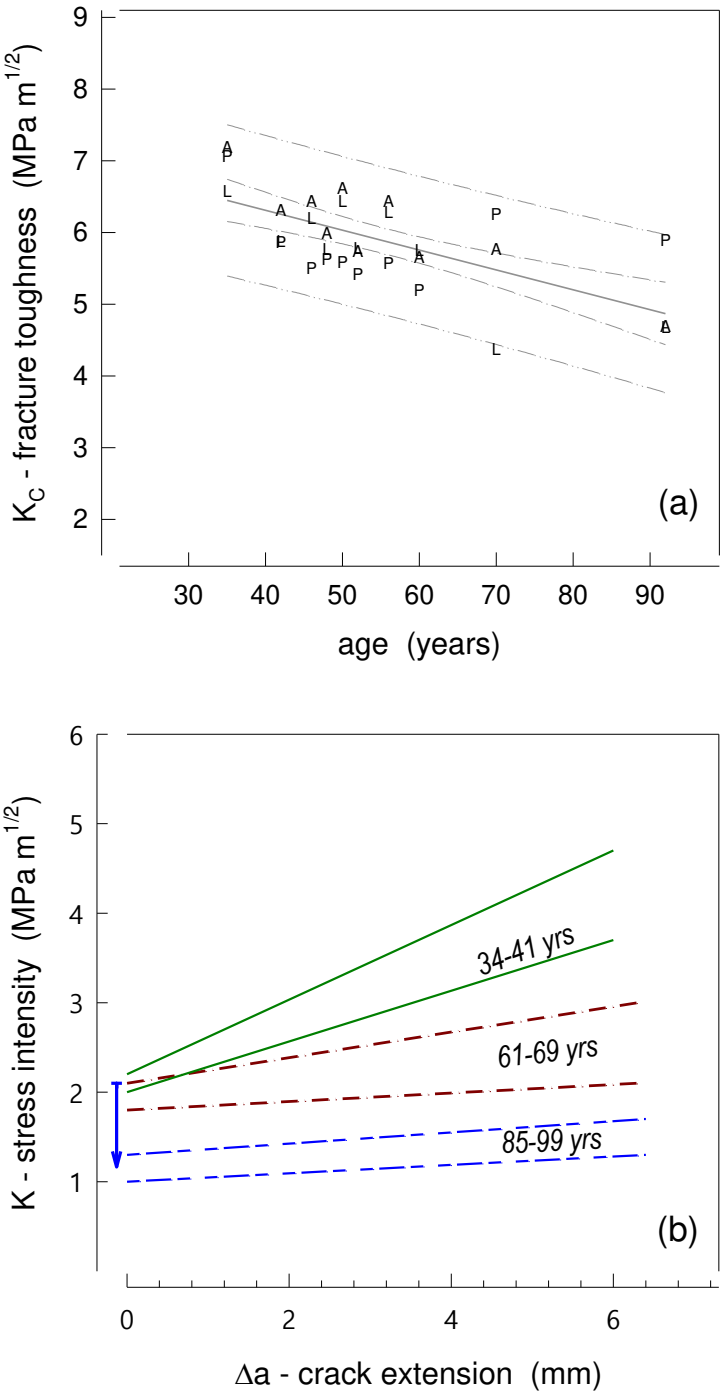

Fig. 3. Crack propagation. (a) The energy required to propagate a crack in the radial (m: microcracking damage), tangential (d: deflected crack) and circumferential (b: brittle fracture) directions in bovine bone with the crack length. Bone is much tougher in the fracture mode accompanied by microcracking damage (m) ahead of it[2, 4]. (b) The energy required to drive a crack across the grain (fibre direction) is an order of magnitude higher than along it[4].

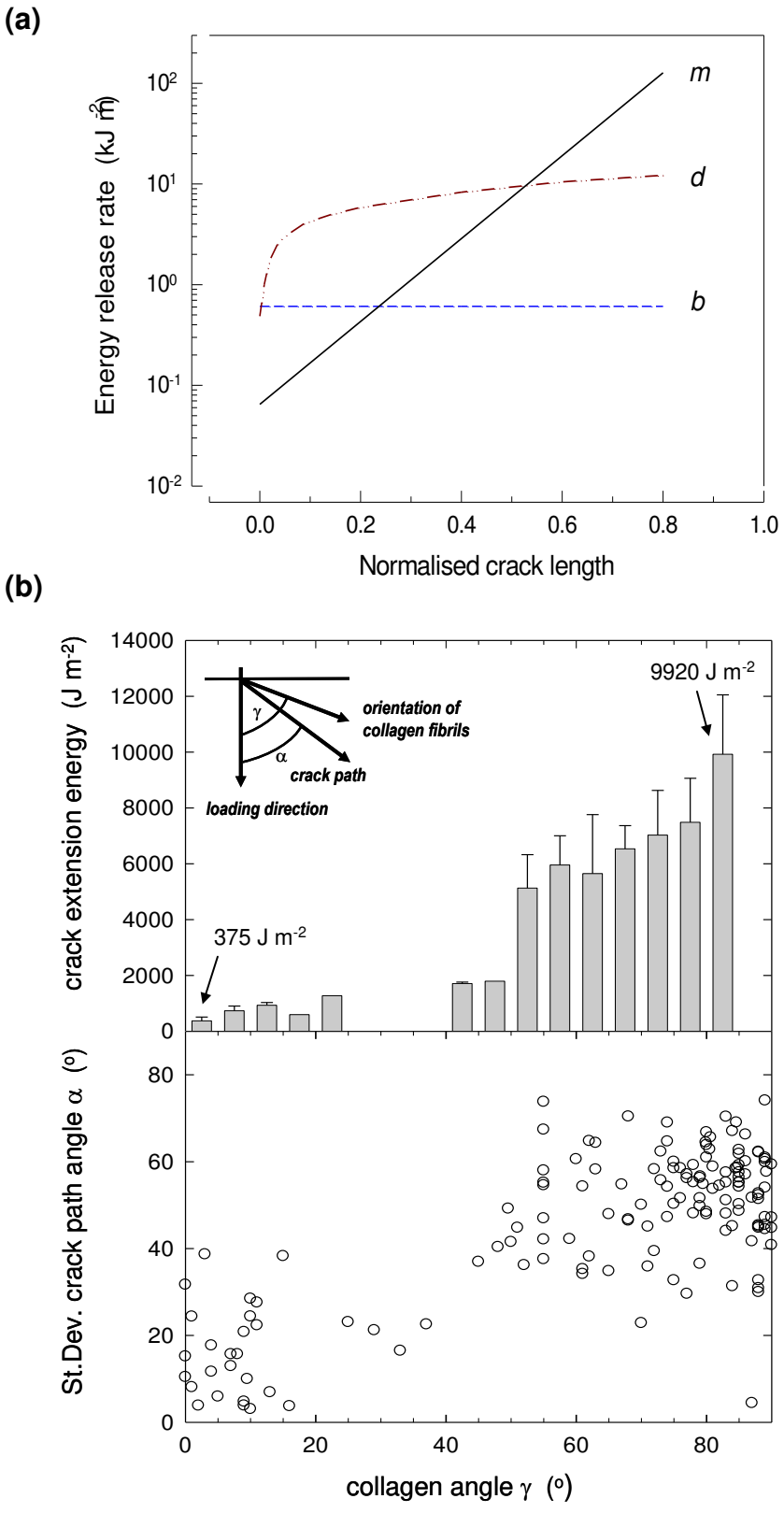

Fig. 4. (a) Work of fracture (slow and controllable mode tests) vs. Impact energy absorption in specimens of human cortical bone of various ages ranging from 4 to 82 yrs old (age as symbol; R^2=0.69). There is a correlation between the two measures, which shows that the underlying cause is the ageing process itself, not the way in which the fracture is quantified[18]. (b) W_f as a function of the stroke rate during the test in 4 bone types: human (unpublished data provided by PZ), tiger, and bovine femurs; and deer antler material[2]. With the exception of antler, the three 'normal' bones experience a ductile-to-brittle transition for stroke rates above 5 mm/min (strain rate: 1.5×10^{-3} s^{-1}). The percentage numbers show what fraction of the specimens achieved a ductile fracture.

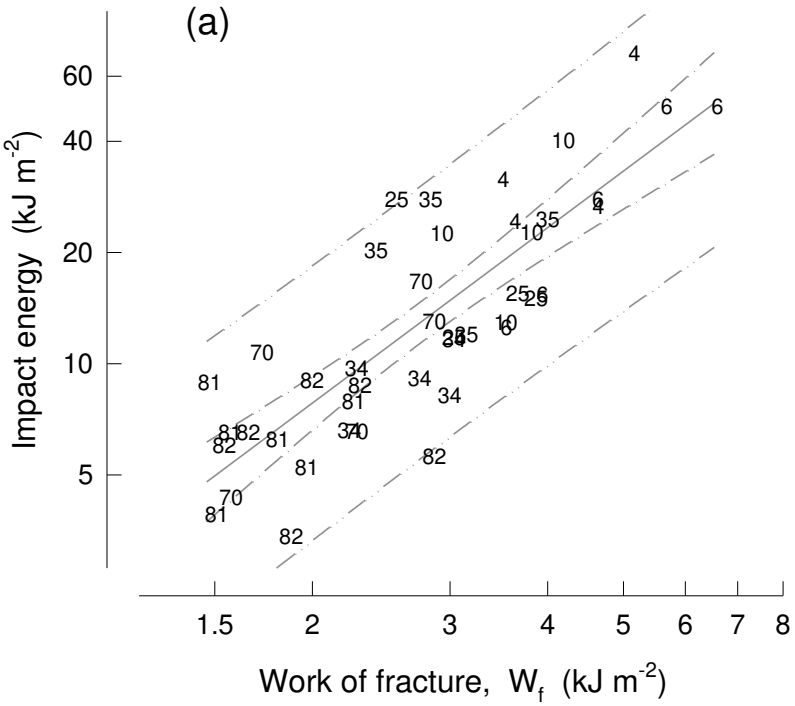

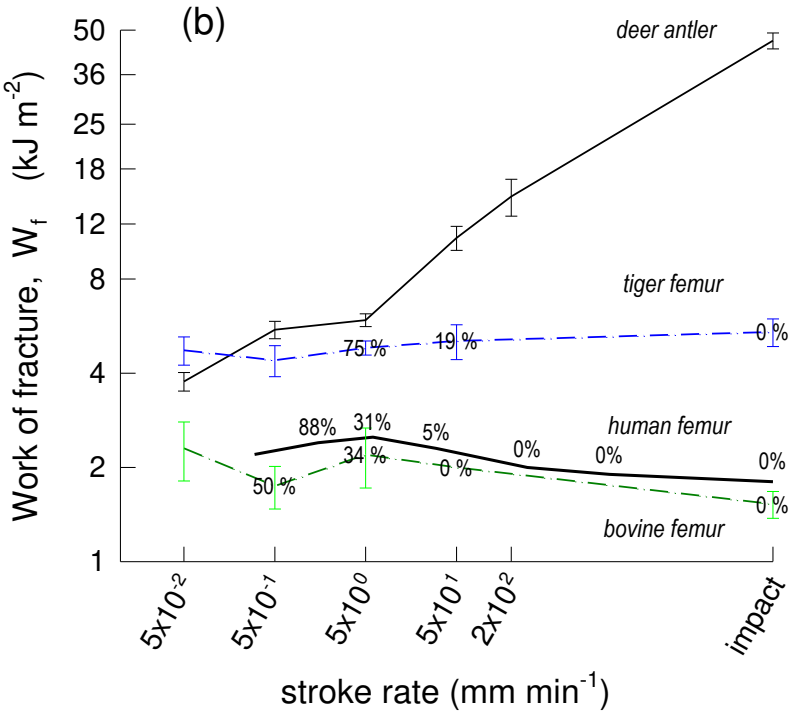
(b)
deer antler
tiger femur
human femur
bovine femur
Work of fracture, W_f (kJ m^{-2})
50
36
25
18
12
8
4
2
1
88%
31%
5%
0%
0%
0%
75 %
19 %
0 %
34 %
0 %
50 %
0 %
5x10^{-2}
5x10^{-1}
5x10^{0}
5x10^{1}
2x10^{2}
impact
stroke rate (mm min^{-1})

Fig. 5. Ductile-to-brittle transition observed in human femoral bone in tension (single pulls to failure, the critical strain rate, for a 10 mm gauge length, is 0.01-0.1 s^{-1}). Above the strain rate threshold the post-yield region, the capacity for energy absorption, and the microcracking damage reduce significantly[18].

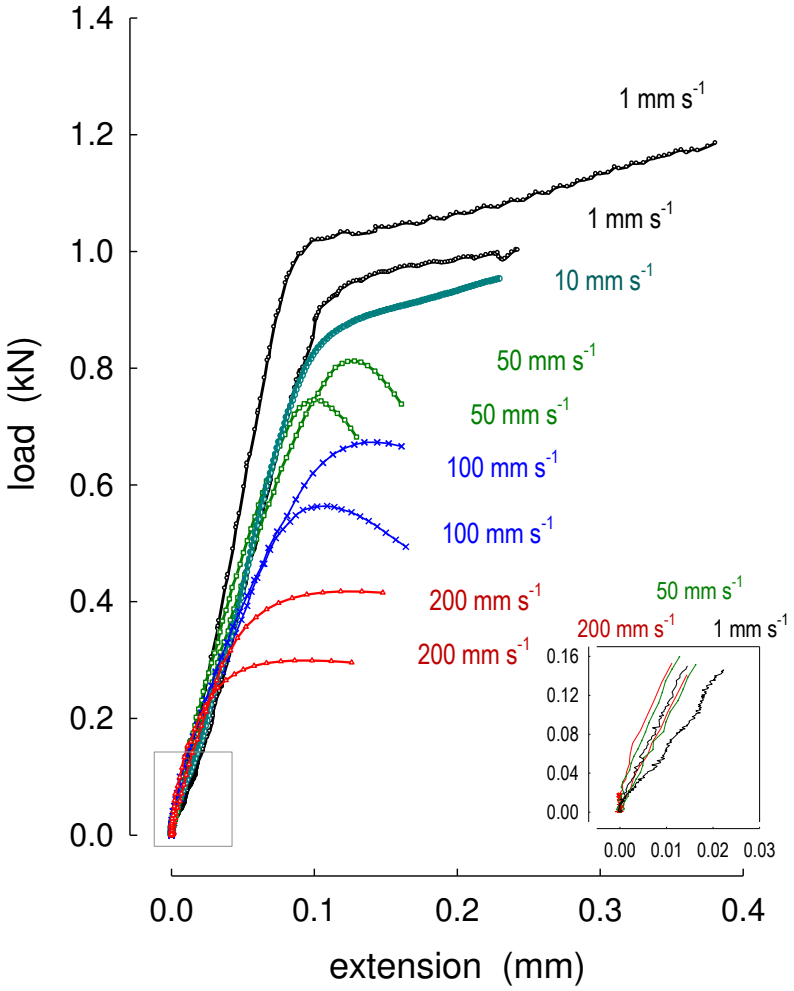

Fig. 6. The growth of cracks is strongly influenced by the structure [135] as shown in a recent article where the separate and added effects of (i) microstructural heterogeneity and (ii) physical characteristics were examined in the fatigue strength of cortical bone in 3 modes :tension, compression and shear. The photo shows a large surface crack which emanated laterally from the fracture surface (on the right of the photo) and grew towards the left advancing naturally between the various bone compartments along boundaries on either side of which the composition and architecture changed sharply.

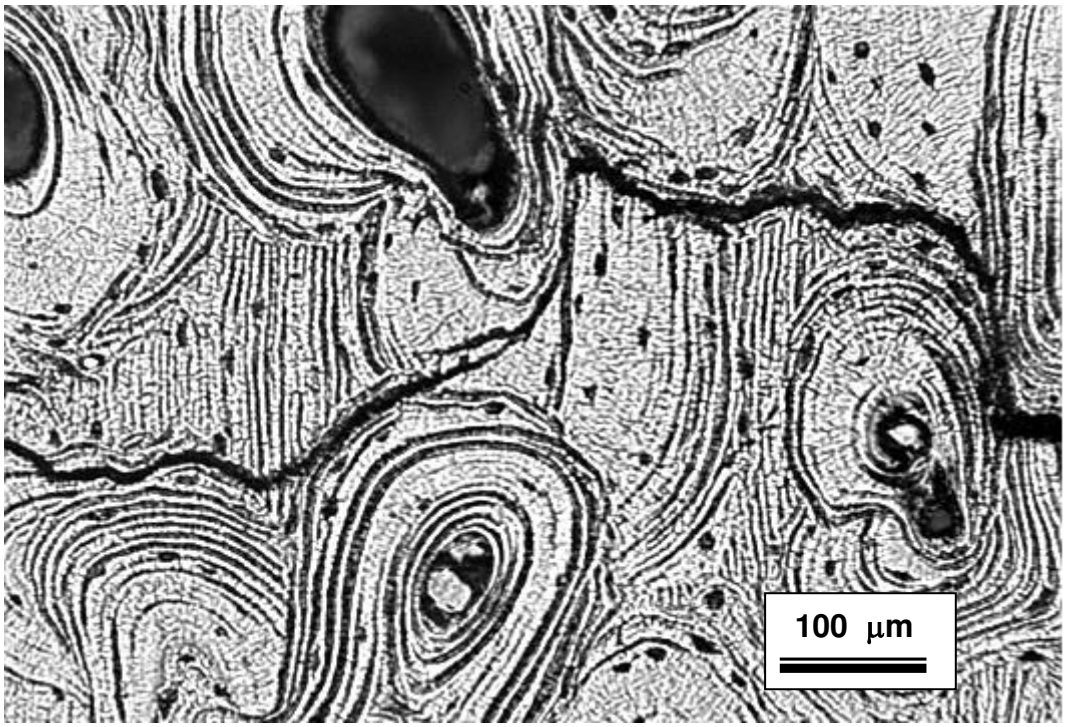

Fig. 7. Lamellar level modulation of mechanics and fiber orientation in bone osteons (Haversian systems) (a) Indentation modulus (stiffness), mapped with 1 μm steps along the radius of an osteon from the femur of a woman shows periodic variations from 24-27 GPa[40]. Scanning electron microscopy image of a typical osteon is shown on the right, with the dashed rectangle indicating the usual width of radial sector used to generate a modulus map. (b) Fibril orientation relative to long axis shows a plywood like[57] radial periodic variation (dashed rectangle), as quantified by scanning microtexture experiments[67, 68]. On average, fibrils are here observed to spiral in a right handed manner around the central blood vessel. On the right, a polarized light microscope image of a typical osteon shows (dashed rectangle) the usual size of the radial sector in which the scans were done. Best fit solid lines (sinusoidal in (a) and exponentially damped sinusoidal in (b)) are meant as guides to the eye.

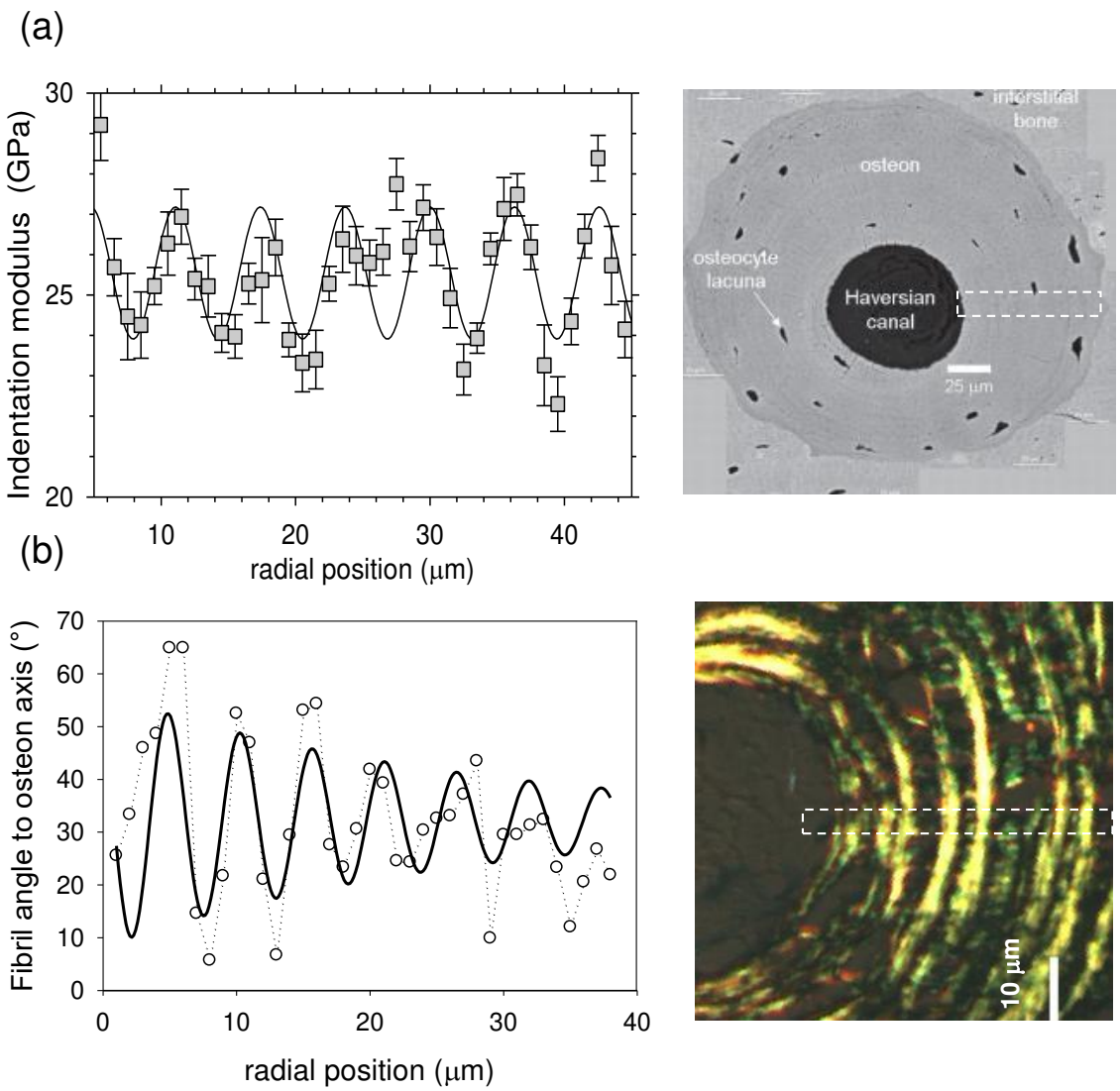

Fig. 8. (a) Schematic view of in-situ tensile testing of bone in the synchrotron [104-106]. High intensity X-ray radiation is used to generate small-angle (SAXS) and wide-angle (WAXD) images of bone nanostructure, concurrently with mechanical deformation. (b) Integrated intensity plots I(q) can quantify fibrillar & mineral structure. On the right, a typical variation of collagen fibril periodicity (D) and width of the meridional reflection (SD) with applied tissue strain is shown.

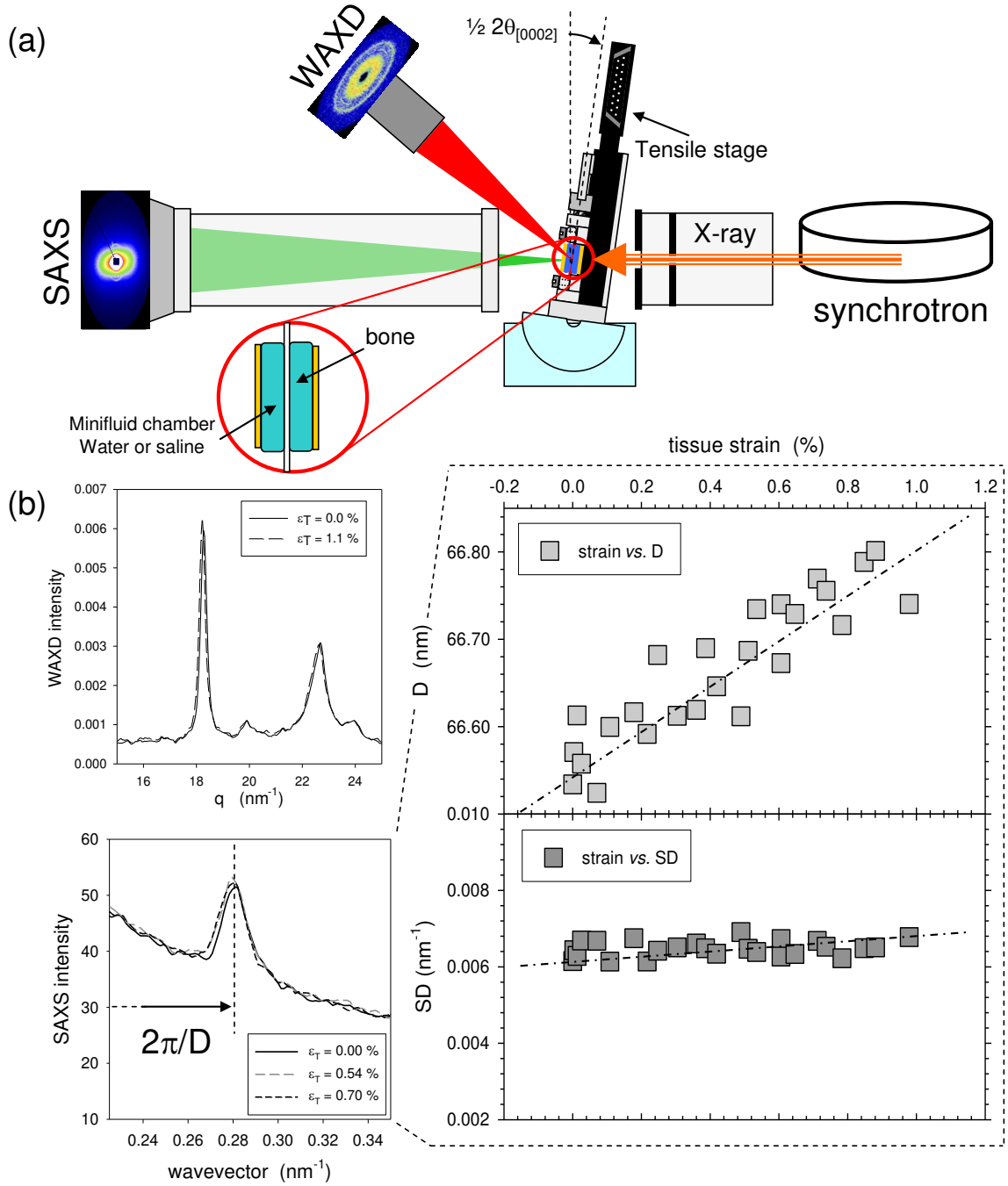

Fig. 9. (a) Fibril (squares) and mineral (circles) strain response to applied tissue strain using in-situ tensile testing with synchrotron diffraction. N=21, error bars are standard deviations. Initial response of fibril and mineral strain is linear, but nonlinearity and plateau behaviour is observed beyond the yield point. Line of equal strains given by dash-dotted line. Data from Gupta *et al.*[105].

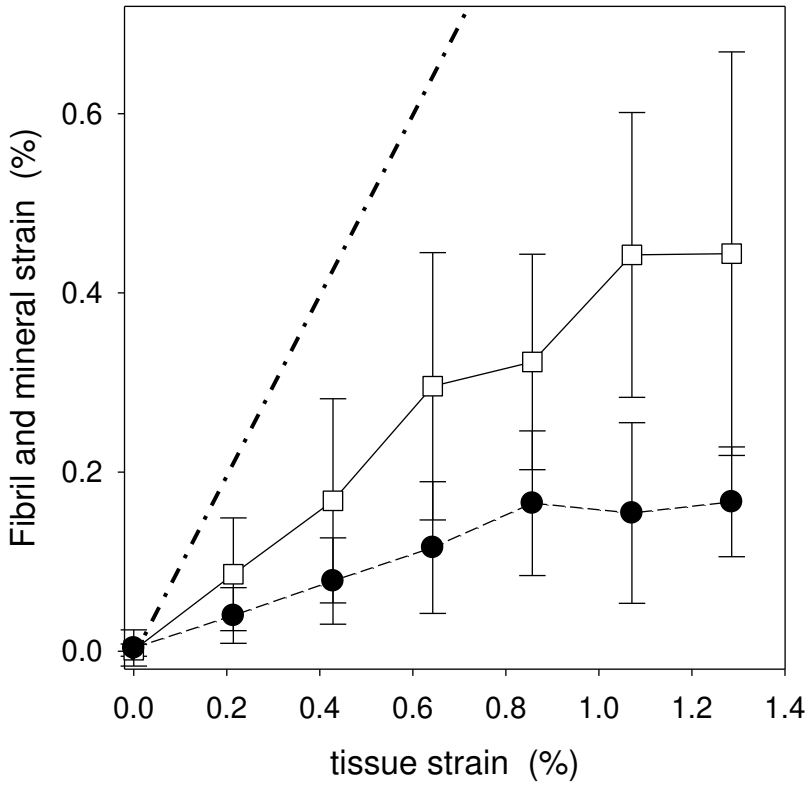

Fig. 10. Tensile strain in bone is transferred in successively lower fractions from the tissue to the nanoscale level on applied external load[105]. Shearing in the intervening soft phase accommodates the remaining strain at each level: in the interfibrillar matrix at the fibril level and in the collagen matrix at the mineral platelet level.

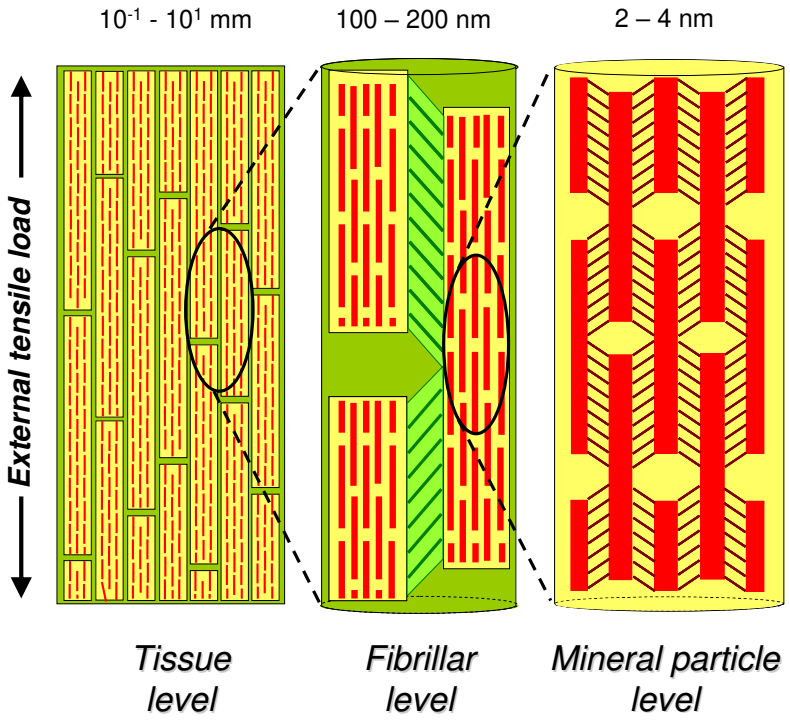

Fig. 11. Two possible schemes for the post yield behaviour at the nanoscale level, which may be different across tissue types and degrees of mineralization. (1) fibrils continue to stretch, possibly heterogeneously, and decouple from the (extrafibrillar) mineral. (2) Mineralized fibrils decouple and slide past each other, and maintain a constant level of fibril strain.

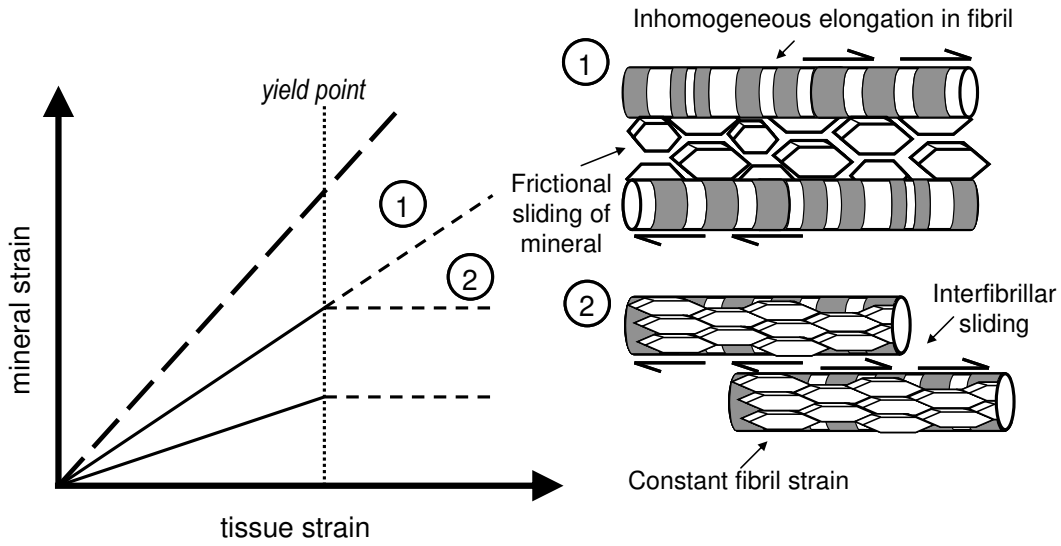

1: Intrafibrillar elongation, mineral mostly extrafibrillar; 2: Interfibrillar sliding, mineral mostly intrafibrillar

Fig. 12. Strain-rate sensitivity of the post yield behaviour of bone. Reducing the stretching velocity from 10 μm s^{-1} to 0.5 μm s^{-1} results in a ~ 10 MPa drop in stress[121]; inset shows that the linear hardening slopes at the different strain rates (shown schematically by the dashed lines) are approximately the same.

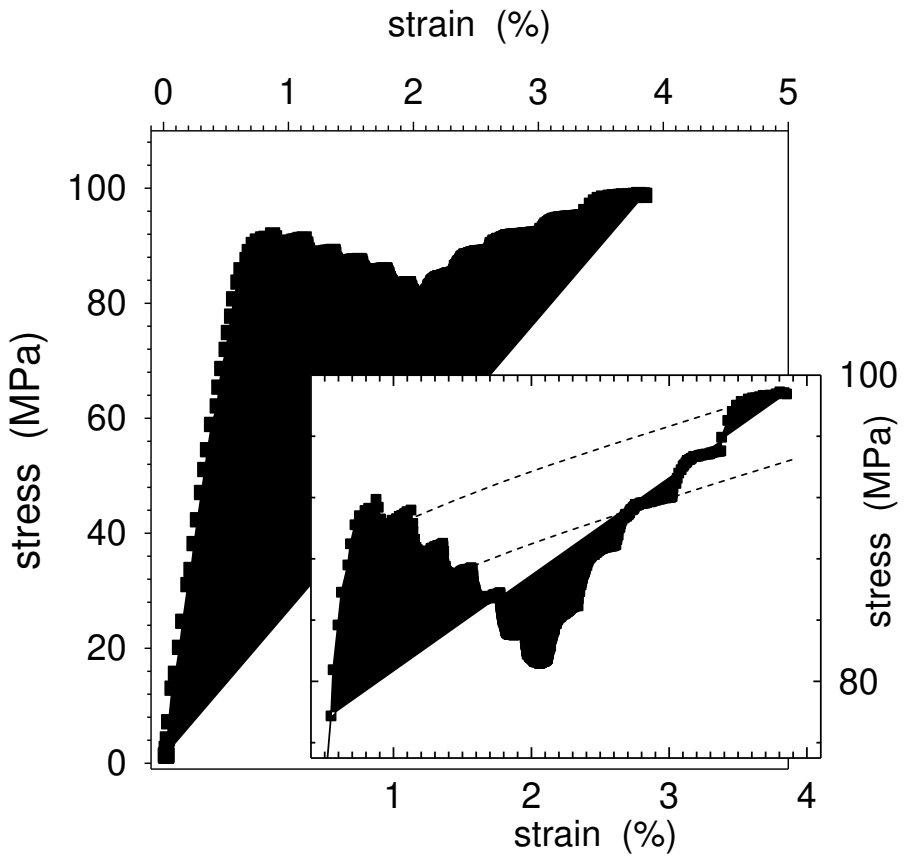

Fig. 13. (a) Two dimensional view of the variation of yield stress σ_Y with temperature and applied strain rate, showing decrease of σ_Y with increasing temperature and decreasing strain rate. N = 63 samples are shown here. (b) One-dimensional view of the same set of data, averaged over each (temperature, strain rate) pair. Data from Fig. 3 in Gupta *et al.*[121].

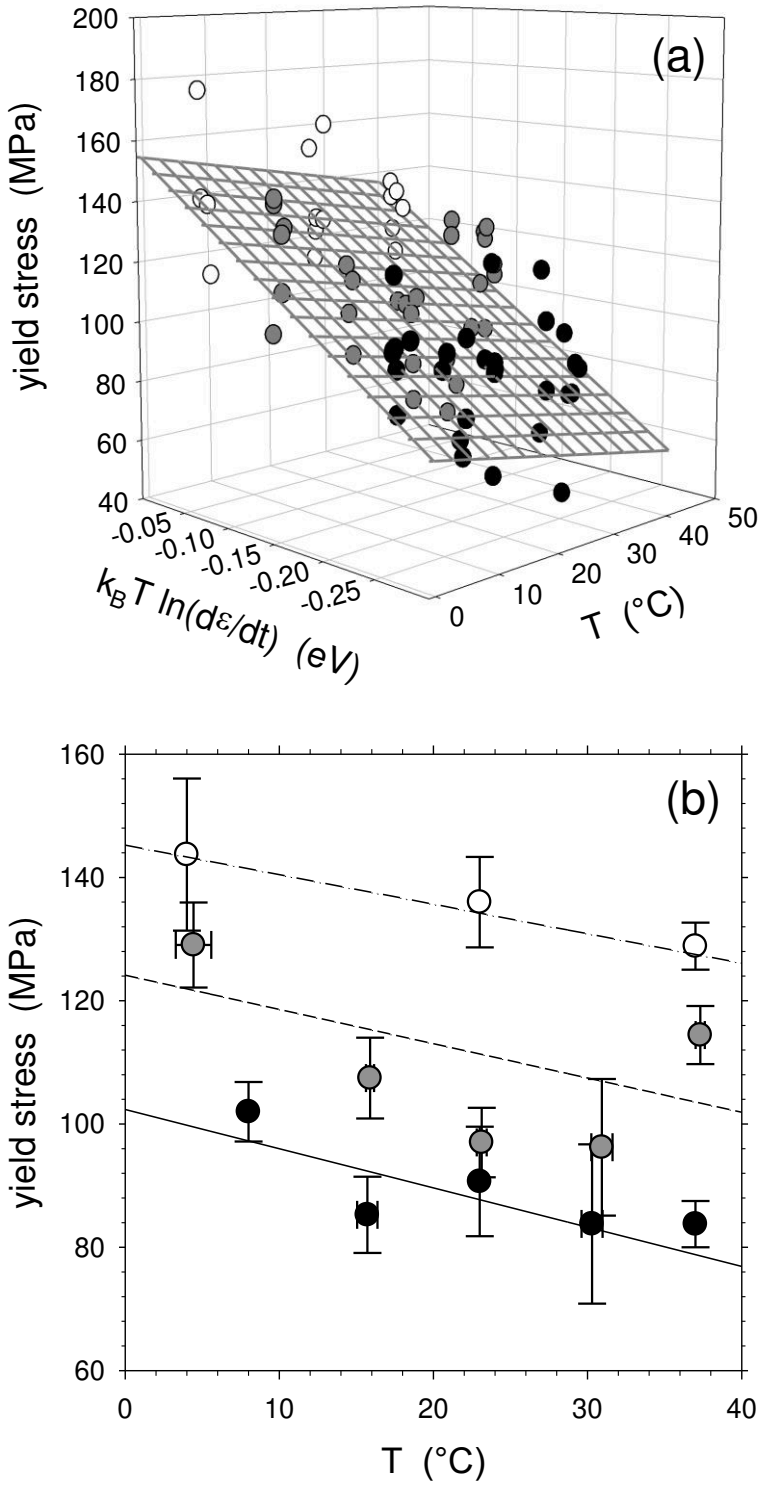

Fig. 14. Schematic of ionic bond breaking in interfibrillar matrix of bone, between negatively charged polyelectrolyte molecules like osteopontin and divalent ions like calcium[121].

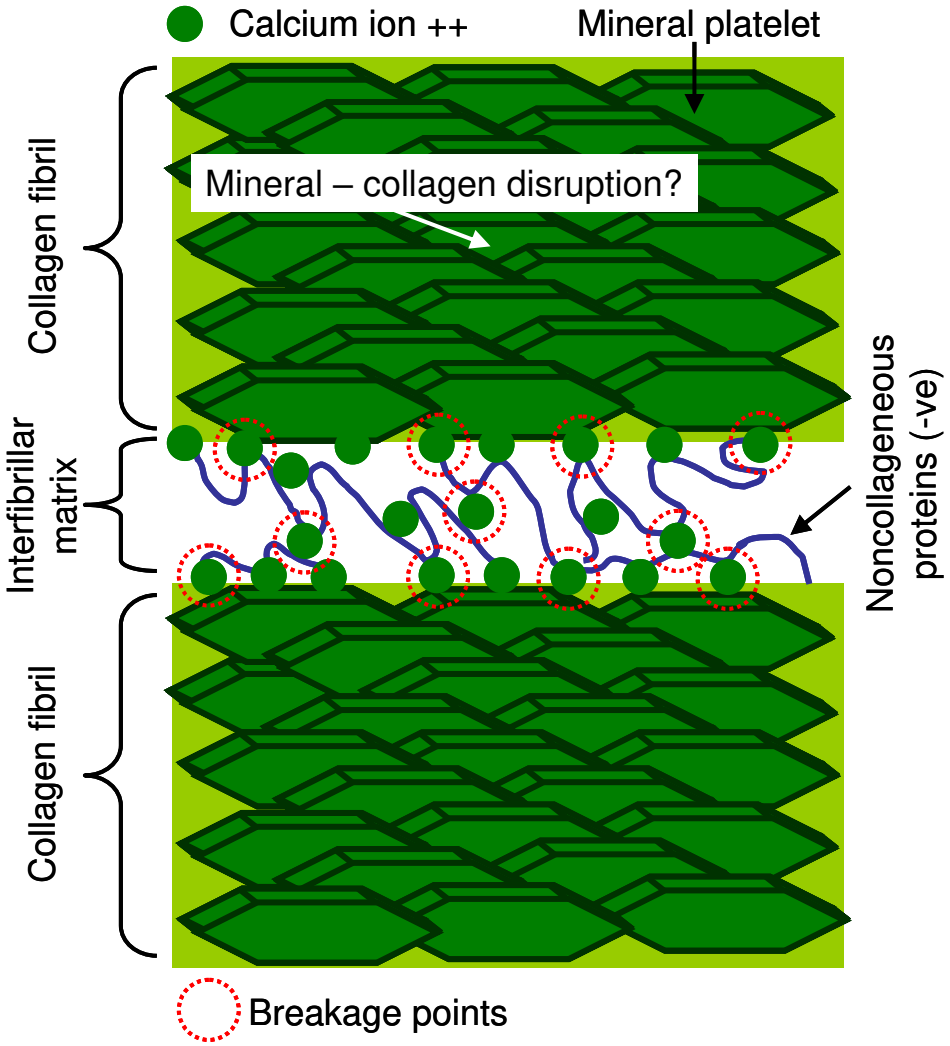

Fracture of bone tissue: the 'hows' and the 'whys'

Gupta, Himadri

2008-10-31

Gupta H, Zioupos P. (2008) Fracture of bone tissue: the 'hows' and the 'whys'. Medical Engineering and Physics, Volume 30, Issue 10, December 2008, pp. 1209-1226
https://doi.org/10.1016/j.medengphy.2008.09.007